Biogeosciences Discuss., 10, 7433–7489, 2013
www.biogeosciences-discuss.net/10/7433/2013/
doi:10.5194/bgd-10-7433-2013

Biogeosciences
Discussions
Open Access

Dissolved Fe across the Weddell Sea and Drake Passage: impact of DFe on nutrients uptake in the Weddell Sea

M. B. Klunder[1,*], P. Laan[1], H. J. W. De Baar[1,2], I. Neven[3], R. Middag[1,], and J. Van Ooijen[4]**

[1]Department of Biological Oceanography, Royal Dutch Institute for Sea Research, Landsdiep 4,1797 SZ Texel, the Netherlands
[2]Department of Ocean Ecosystems, University of Groningen, Kerklaan 30 ,9751 NN Haren, the Netherlands
[3]Department of Plant Physiology, University of Groningen, Kerklaan 30, 9751 NN Haren, the Netherlands
[4]Department of Chemical Oceanography, Royal Dutch Institute for Sea Research, Landsdiep 4,1797 SZ Texel, the Netherlands
[*]now at: Dutch board for the authorisation of biocides and plant protection produces, Wageningen, the Netherlands
[**]now at: Department of Chemistry, University of Otago, Otago, New Zealand

Received: 10 March 2013 – Accepted: 15 March 2013 – Published: 29 April 2013

Correspondence to: M. B. Klunder (maartenklunder@hotmail.com)

Published by Copernicus Publications on behalf of the European Geosciences Union.

BGD

10, 7433–7489, 2013

Abstract

This manuscript reports the first full depth distributions of dissolved iron (DFe) over a high resolution Weddell Sea and Drake Passage transect. Very low dissolved DFe concentrations (0.01–0.1 nM range) were observed in the surface waters in the Weddell Sea, and within the Polar regime in the Drake Passage. Locally, enrichment in surface DFe was observed, likely due to recent ice melt (Weddell Sea) or dust deposition (Drake Passage). In the Weddell Sea, the low DFe concentrations can be partly explained by high POC export and/or primary production (indicated by chlorophyll fluorescence). As expected, in high DFe regions a strong silicate drawdown compared to nitrate drawdown was observed. However, this difference in drawdown between these nutrients appears not related to biological activity on the Peninsula shelf. In the Western Weddell Sea transect, with relatively small diatoms, no relationship between N:P and N:Si removal ratios and DFe was observed. For comparison, nutrient depletion is also presented for a transect along the Greenwich Meridian (Klunder et al., 2011), where diatoms are significantly larger, the N:P and N:Si removal ratio increased with increasing DFe. These findings confirm the important role of DFe in Southern Ocean (biologically mediated) nutrient cycles.

Over the shelf around the Antarctic Peninsula, higher DFe concentrations (>1.5 nM) were observed. These elevated concentrations of Fe were transported into Drake Passage along isopycnal surfaces. At the South American continent, high (>2 nM) DFe concentrations were caused by fluvial/glacial input of DFe.

On the Weddell Sea side of the Peninsula region, formation of deep water (by downslope convection) caused relatively high Fe (0.6–0.8 nM) concentrations in the bottom waters relative to the water masses at mid depth (0.2–0.4 nM). During transit of Weddell Sea Bottom Water to Drake Passage, through the Scotia Sea, extra DFe is taken up from seafloor sources, resulting in highest bottom water concentrations in the southernmost part of the Drake Passage of >1 nM. The Weddell Sea Deep Water concentrations

(∼ 0.32 nM) were consistent with the lowest DFe concentrations observed in Atlantic AABW.

1 Introduction

It is now well established that phytoplankton growth in the High-Nutrients Low Chlorophyll (HNLC) Southern Ocean is severely limited as a result of low Fe concentrations (De Baar et al., 1990; Buma et al., 1991; De Baar et al., 1995, 1999) in combination with light limitation due to deep mixing (Mitchell et al., 1991; Lancelot et al., 2000; De Baar et al., 2005) as well as photo-inhibition (Alderkamp et al., 2010, 2011), and possibly also with (co-)limitation of other metals like Mn (Middag et al., 2013). Although there have been very little deep water values of dissolved Fe in the Weddell Sea reported in the literature (De Jong et al., 2012), several studies have reported dissolved Fe values in the upper waters (Sanudo-Wilhelmy et al. 2002; Lannuzel et al., 2008; Lin, 2011).

North of the Antarctic Peninsula, the ∼ 800 km wide Drake Passage is the narrowest opening between Antarctica and the South American continent. The eastward flowing Antarctic Circumpolar Current (ACC) is forced through the narrow Drake Passage, resulting in strong velocities (Sokolov and Rintoul, 2007). Thus far no data did exist for dissolved Fe in the complete deep water column of the Drake Passage. However in the upper water column the distribution of (dissolved) iron (DFe) in the region around the Antarctic Peninsula is relatively well studied in recent years (Sanudo-Wilhelmy et al., 2002; Lin et al., 2011). Some studies focus specifically on the peninsula region because of the important role that Fe plays in the phytoplankton blooms observed close to the Peninsula and further east, following the main currents (Dulaiova et al., 2009; Ardelan et al., 2010).

The GEOTRACES program of the International Polar Year 2007–2008 was designed to produce the first-ever deep ocean sections of dissolved Fe (DFe) and other (bio-essential) trace metals in the polar oceans. The expedition ANT/XXIV/3 aboard icebreaker R/V *Polarstern* in 2008 (Fahrbach et al., 2011) comprises the two first deep sections of dissolved Fe across the Weddell Sea and Drake Passage, respectively, reported here and also in relation with a complete deep section of dissolved Fe along the Greenwich meridian (Klunder et al., 2011).

There are several input sources of Fe to the surface waters of the Southern Ocean. Possibly the most important is the supply from below of (Fe rich) deep waters (De Baar et al., 1995 (their Table 1); Löscher et al., 1997; Hoppema et al., 2003; Croot et al., 2004; Klunder et al., 2011). Atmospheric dust deposition is deemed to be very low in this region (Jickells et al., 2005) and melting of free floating icebergs, that previously were grounded on shelves and carry sediments, supplies Fe to surrounding waters (Löscher et al., 1997; Lin et al., 2011). Both atmospheric dust input and iceberg melting are episodic, and a challenge to assess in a basin wide or annual supply estimate. Nevertheless, the modelling results from Raiswell (2011), indicated that input of bio available Fe to the Weddell Sea by icebergs may be as large as total dust input (5.6×10^5–1.8×10^7 mol Fe/100 days melting). Rare events of dust deposition were observed along the Greenwich Meridian (Klunder et al., 2011; Middag et al, 2011a; 2011b). Anoxia in pore waters of shelf sediments causes dissolution of reduced Fe (Elrod et al., 2004), some of which by either sediment resuspension (Luther and Wu, 1997) and/or eddy diffusion enters overlying waters. Upon entrainment and mixing these Fe enriched shelf waters were found around and beyond the Antarctic Peninsula (Dulaiova et al., 2009) and near island archipelago's like the Kerguelen plateau (Bucciarelli et al., 2001; Blain et al., 2007; Chever et al., 2010) and Crozet islands (Planquette et al., 2007). In the Drake Passage, eddy activity may involve both upwelling and downwelling and thereby influence the distribution of DFe (Kahru et al., 2007). Phytoplankton blooms observed at and close to the Antarctic Peninsula shelf regions may be explained by the delivery of shelf derived DFe. There are several lines of evidence that limited availability of DFe for phytoplankton may influence the uptake ratio of nutrients in the Southern Ocean (De Baar et al., 1997; Takeda, 1998; Marchetti and Cassar, 2009). Upon Fe deficiency the cellular N content decreases due to impairment of Fe-requiring enzymes nitrate reductase and nitrite reductase required for ultimate production of amino acids, i.e. protein content of cells decreases. This implies a lower N/P element ratio of plankton. For diatoms, that generally continue to produce the opaline (SiO_2) frustules, this implies a lowering of their overall N/Si content (Takeda et al., 1998 and overview by Marchetti and Cassar, 2009). Moreover, Hoppema et al. (2007) have shown less Si removal relative to C removal and less Si removal relative to N removal in the surface waters approaching the Peninsula region, which they attributed to increasing DFe availability.

In the deep waters, the North Atlantic Deep Water (NADW) enters the ACC at ~2000–3000 m depth (Klunder et al., 2011). This iron-rich water mass (Fe = ~0.7 nM) eventually flows into the Weddell Sea as Warm Deep Water (WDW). In the Weddell Sea, this water becomes incorporated in the Weddell Gyre System. The return flow to the ACC consists of Weddell Sea Bottom Water (WSBW) and Weddell Sea Deep Water (WSDW). Although the exit of WSDW is arguably the main contributor to the ACC water, at the Scotia Ridge, the WSBW is an important water mass leaving the Weddell Gyre northwards over the Scotia Ridge, into the Scotia Sea and further north over the worlds abyssal oceans as Antarctic Bottom Water (AABW) (Naveira Garabato et al., 2002). The deep Drake Passage is dominated by Circumpolar Deep Waters which contain generally ~0.4–0.5 nM DFe (Klunder et al., 2011). However, at ~2000 m depth at the Patagonian Continental Shelf, an additional water mass derived from the East Pacific Ocean, carrying hydrothermal origin properties (Well et al., 2003, Sudre et al., 2011) was observed.

In this study we present the distribution of dissolved (<0.2 µm fraction) iron (DFe) over two combined transects, one crossing the Weddell Sea and one crossing the Drake Passage. The first transect comprised 8 stations in the Weddell Sea, from the Central Weddell Sea (17° E) towards onto the Antarctic Peninsula shelf close to Joinville Island (Fig. 1a). The other transect stretched from Elephant Island (Fig. 1b), situated on the shelf, Northeast of the Antarctic Peninsula, to Drake Passage.

The simultaneous sampling for trace metals (Middag et al., 2011a, b; 2012), major nutrients (Si, NO_3, PO_4), biological parameters (Rutgers van der Loeff et al., 2011;

BGD
10, 7433–7489, 2013

Neven et al., 2011) and physical parameters (Fahrbach et al., 2011) allows to investigate the input of DFe from the Antarctic Peninsula to the surrounding waters in the Weddell Sea and in Drake Passage and to give an estimation of the relative nutrient removals in relation to DFe concentrations. Moreover, other sources and sinks of DFe in the Weddell Sea and Drake Passage are discussed. The DFe data here presented were collected in March 2008, thus towards the end of the vegetative season, when DFe may have become depleted and limiting for phytoplankton growth (Sedwick et al., 2000). This would be reflected in nutrient removal in the months prior to our occupation of the transects. Using the deficit between the remnant winter water and the surface waters an estimation of this nutrient removal can be made (Hoppema et al., 2007). Here we present estimates for such removal and investigate their relation with DFe availability.

2 Methods

2.1 Sampling and analysis

Water samples were collected during the ANT XXIV / 3 expedition of RV Polarstern between March 15 and April 12, 2008 (Fig. 1a). Samples were taken and analysed under ultraclean conditions extensively described by De Baar et al. (2008) and (Klunder et al., 2011). Seawater was filtered over a 0.2 µm filter cartridge (Sartrobran-300, Sartorius) under nitrogen pressure. For each depth, replicate samples of DFe were taken in 60 ml HDPE sample bottles and acidified to pH = 1.8 with 12 M HCl (Baseline, Seastar Chemicals) and left overnight. All bottles, used for storage of reagents and samples, were acid cleaned according to a three step cleaning procedure, as described by Middag et al. (2009). We ensured all the Fe was in the Fe (III) form, by adding 60 µl of 1 ‰ hydrogen peroxide (Merck suprapur 30 %), at least one hour before measurement. The DFe was measured using flow injection analysis with luminol chemiluminescence, where DFe was pre-concentrated on an IDA Toyopearl AF-Chelate resin (Klunder et al.,

BGD
10, 7433–7489, 2013

2011). After pre-concentration, the column was rinsed (60 s) with de-ionized ultrapure (DI) water (18.2 MΩ) and subsequently Fe was eluted from the column (120 s) using 0.4 M HCl (Merck Suprapur). Pre-concentration time was usually 120 s.

2.2 Calibration and validation

The system was calibrated using standard additions of Fe to low DFe seawater. For all samples a duplicate sample was taken. For outlying values, profiles of the other trace metals dissolved aluminium (DAl) and manganese (DMn) as well as nutrients and physical parameters (e.g. light-transmission) were evaluated for consistency. In case no deviations were observed in the other physical, chemical and biological parameters and both the initial and duplicate sample showed an exceptional value, the exceptional data point was considered as erroneous if the value deviated more than +25 % from the expected profile based on linear interpolation between the DFe-concentration in the seawater samples above and below the data point (after Middag et al., 2011a, b and Klunder et al., 2011). Any truly elevated DFe concentration would be reflected in the corresponding chemical or physical parameters, therefore this is considered an acceptable approach regarding outlying values. Each sample was analysed three times (three peaks) and standard deviation was generally below 5 %.

Regularly the combined blank of the 1 min MQ-column wash and the 0.4 M HCl for elution of the column was calculated from the amount of counts measured upon zero (0) seconds loading time. The average value for this blank was 14 ± 11 pmol ($n = 18$) and this blank did not exceed 40 pM. By double versus single addition of the H_2O_2 it was found that this did not cause a quantifiable blank. The contribution of the Seastar Baselines Hydrochloric Acid is deemed to be negligible (0.04 pM/sample; see Klunder et al., 2011). The detection limit was determined regularly and defined as the standard deviation of 5 peaks of 10 s loading of low-Fe seawater (subsurface minimum), multiplied by 3. Average detection limit was typically 9 ± 5 pM Fe ($n = 7$), and the detection limit did not exceed 17 pM Fe. Therefore, in this study, all values <0.01 nM are presented as 0.01 nM.

In order to validate the accuracy of the system, standard reference seawater was measured regularly, in triplicate. There is SAFe surface (S) water and SAFe deep (D2) water available to validate against different ranges of Fe concentration (Johnson et al., 2007). The average concentrations we found were 0.085 ± 0.023 nM (n = 16) and 0.958 ± 0.039 (n = 13) for SAFe S and SAFE D2 respectively. These results are consistent with the community consensus values 0.094 ± 0.008 for SAFe S and 0.923 ± 0.029 nM for SAFe D2 (www.geotraces.org, datasheet version November 2011).

In order to investigate the relationship between DFe and net nutrient removal in the Weddell Sea the seasonal nutrient uptake in the upper layer above the Winter Water is calculated. This method and the assumptions needed are described in more detail by Hoppema et al. (2002, 2007). Briefly, the difference in nutrient concentration between the Winter Water (subsurface θ minimum <-1.6 ° C) and the overlying surface water was calculated. Next, upon vertical integration over the upper layer depth interval, the net seasonal nutrient removal from the upper layer, relative to the winter water is obtained. In order to correct for spatial variations in diluting meltwater, concentrations are normalized to a salinity of 34.5. For comparison, also the net removal for the stations situated within the Weddell Gyre at the Greenwich Meridian at 0° W (Klunder et al., 2011) were included. The stations with a distinct Winter Water layer, allowing nutrient removal calculation, were situated between 60–69° S at the Greenwich meridian and between 17–48.5° W in the west Weddell Sea transect and are marked by the two shaded area's in Fig. 1a. Moreover, for discussion of the relation between DFe and nutrients, also the phytoplankton community in our stations is studied. Stations for which phytoplankton data is available are marked with a "B" in Fig. 1a. More details on the phytoplankton data can be found in (Neven et al., 2011).

2.3 Hydrography

Transport of water masses in the Weddell Sea is dominated by the Weddell Gyre, a cyclonic current, with its westward component near the Antarctic continent and an

Discussion Paper | Discussion Paper | Discussion Paper | Discussion Paper |

BGD

10, 7433–7489, 2013

Dissolved Fe across the Weddell Sea and Drake Passage

M. B. Klunder et al.

eastward component along Bouvet Ridge (Fig. 1a; Klatt et al., 2005; Fahrbach, 2004). Although the whole Weddell Sea is influenced by the gyre, the strongest velocities are observed close to the continental shelves (Fahrbach et al., 1994). The Weddell Sea is dominated by five water masses distinguished on the basis of potential temperature (θ) and salinity (after Klatt et al., 2005). In the upper surface, the low salinity (<34.6) Antarctic Surface Water (AASW) is found. As remnant of the preceding winter, a θ minimum marks the Winter Water (WW) layer at ~100 m depth (Fig. 2a). Below the Winter Water, Warm Deep Water (WDW) is found. This water enters the Weddell Gyre from the Antarctic Circumpolar Current in the North, and carries the Lower Circumpolar Deep Water properties (θ >0 ° C; Sal >34.6) (Fig. 2a). The most voluminous water mass in the Weddell Sea is the slightly colder Weddell Sea Deep Water (–0.7 ° C <θ <0 ° C) which is observed from ~1500 m to ~4000 m depth. The western part of the Weddell Sea is known as an important region for bottom water formation. Intense cooling of surface waters causes loss of buoyancy and subsequent sinking along the Peninsula slope (Huhn et al., 2008), resulting in the formation of Weddell Sea Bottom Water (WSBW) (θ <-0.7 ° C) (Fig. 2a). Both the latter WSBW and the WDW influence the WSDW through overall vertical mixing. Eventually, the WSDW and WSBW leave the Weddell Sea and extend further Northwards as AABW (Klatt et al., 2005; Orsi et al., 1993; Naveiro Garabato et al., 2002). The magnitude of these processes is considerable; estimations of WSDW and WSBW outflow are from 8–9 to 11 Sv (1 Sv is $10^6\ m^3\ s^{-1}$; Orsi et al. 1993; Naveiro Garabato et al., 2002; Klatt et al. 2005). Not all inflowing Warm Deep Water ends up as WSDW and leaves the Weddell Gyre as AABW; upwelling of deep waters and subsequent Ekman transport causes a loss of water at intermediate depths that eventually flows equatorwards as Antarctic Intermediate Water (AAIW). This process has important consequences for the biogeochemical composition of the surface waters in the Subantarctic Zone (Hoppema et al., 2003). Within the Weddell Sea, the σ_θ – plot shows slightly denser water in Central Gyre, and somewhat less dense water closer to the ridges. Also relatively lighter water is seen along the slope (Fig. 3a).

BGD
10, 7433–7489, 2013

Title Page
Abstract | Introduction
Conclusions | References
Tables | Figures
◄◄ | ►►
◄ | ►
Back | Close
Full Screen / Esc
Printer-friendly Version
Interactive Discussion

The Drake Passage is marked as the passage where the major Southern Ocean fronts are very near to each other because of its narrow extent. At the Drake Passage, the Antarctic Circumpolar Current (ACC) approaches the continental shelves, bounded by the Subantarctic Front (SAF) at 55.6° S in the North and the Southern Boundary of the ACC (SB-ACC) at 60.4° S in the South. Within the ACC, the Polar Front (PF) is found at 57.3° S (defined as the northernmost extent of the 2° C subsurface θ minimum (Pollard et al., 2002)). Here, it is clearly visible that the colder, more saline water subducts as AAIW under warmer waters (Fig. 2b). Southwards of the SB-ACC, near the Antarctic Peninsula, the Weddell Scotia Confluence Zone is found. Sudre et al. (2011) distinguished the different water masses in the Drake Passage using multiparametric analysis. Briefly, in the surface waters in the southern part of the transect (south of 58.5° S), the Antarctic Surface Water (AASW) was observed to a maximum depth of ~ 100 m. North of 58.5° S, the Subantarctic Surface Water (SASW) reaches from the surface to a maximum of 700 m depth at the Patagonian side. Winter Water (WW) was observed over most of the transect, at a depth of 200–300 at 56° S to ~ 100m at 60° S (Fig. 2b). Antarctic Intermediate Water (AAIW) followed a downward path; from 300–600 m at the Polar Front, to 800–1200 m depth at the Patagonian shelf (Fig. 2b). This pattern of water masses shoaling towards the south is also observed in the Circumpolar Waters below. The Upper Circumpolar Water (UCDW) and Lower Circumpolar Water (LCDW) were observed from ~ 1200–2200 m and ~ 2200–4000 m respectively at the Patagonian Shelf, and found up to ~ 150–700 m and ~ 700–3000 m, respectively, south of the Polar Front. South of 58° S, the Weddell Sea Deep Water (WSDW) was observed as a 500 m thick bottom layer (Fig. 2b). Close to the Patagonian shelf (55–56.5° S), at ~ 2000–3000 m depth, an additional deep water mass is identified by high δ^3He concentrations. This water mass, named Southeast Pacific Deep Slope Water (SPDSW) was earlier reported by Well et al. (2003) and for this cruise by (Sudre et al., 2011) and (Middag et al., 2012). It originates from the South Pacific. The Drake Passage is known for the occurrence of mesoscale eddies. Locally, these eddies may be of major importance for the transport of trace elements, as reported for dissolved

BGD
10, 7433–7489, 2013

Zn (Croot et al., 2011) and iodate (Bluhm et al., 2011). The position of the fronts as well as the pattern of water masses, shoaling to the south, are clearly visible from the sigma-theta plot (Fig. 3b).

3 Results

The distribution of DFe in the Weddell Gyre is depicted in Fig. 4a and b. Generally, the DFe concentrations within the Weddell Sea surface waters were very low, ranging from <0.01 nM (Lowest Limit of Detection; LLoD) to 0.1 nM. Exceptions to this pattern wre slightly higher concentrations (0.12–0.17 nM) at the upper surface (10 m depth) at 27° W, and in the upper 50 m at 48° W. Although there was little increase in DFe in the upper 100 m towards the Pensinsula, concentrations show a sudden increase between 200 and 600 m near the shelf break. In the southeast and northwest part of the Weddell Sea transect, concentrations in the WDW were 0.2–0.3 nM, whereas in the Central Weddell Sea, even lower concentrations (0.1–0.2 nM) were observed. Below the WDW, in the Weddell Sea Deep Water, concentrations start to increase with increasing depth to values of 0.2–0.4 nM. The lowest concentrations in the WSDW are observed in the centre of the Gyre, and slightly higher values in the direction of the shelves. These WSDW concentrations are relatively low for deep water concentrations in the Southern Ocean (Klunder et al., 2011; Tagliabue et al., 2012). Below 4000 m, at most stations WSBW was observed, with slightly higher DFe concentrations, likely as a result of deep water formation along the shelf.

The distribution of DFe in the Drake Passage is depicted in Fig. 5a and b. In the Drake Passage, strong fluctuations were observed in the DFe concentration in the surface waters. Close to the Peninsula the DFe concentrations reach 1–2 nM, with a maximum in the subsurface, 100–200 m, depth range. Further north, surface concentrations were low (<0.2 nM), but an enrichment in DFe was observed at 58.3° S (station 238), corresponding to high Al concentrations (Middag et al., 2012). At the Northern end of the transect, close to Tierra de Fuego, DFe enrichment corresponded with enrichment of

DMn and DAl and low salinities (Middag et al., 2012). In the Drake passage, the DFe increase with depth is stronger than that in the Weddell Sea; concentrations >0.25 nM were observed from 25–200 m in the Southern Drake Passage, and from below 400 m in the Northern Drake Passage (WW and AAIW, see Sect. 3). Below this, low DFe concentrations followed an ascending pattern towards the south, from ~57.5° S to 60° S, as also observed in DMn and typical for the water mass distribution in the Drake Passage (Middag et al., 2012; Sudre et al., 2011). The most northerly station, situated above the Patagonian shelf had very high DFe concentrations (2.64 nM at 25 m) in the upper surface sample. Deeper in the water column, onto the continental shelf, a strong, local, maximum in DFe (>1.5 nM) was observed at ~2500 m depth. This maximum was consistent with the presence of South Pacific Deep Slope Water (SPDSW), originating from the Central South Pacific, carrying a hydrothermal signal (see Sect. 3) (Middag et al., 2012; Sudre et al., 2011). The DFe data, along with physical and station information is to be found in the online electronic supplement data Table S1.

The nutrient removals for the Weddell Sea and Greenwich meridian stations are shown in Fig. 6. There was a strong fluctuation in the summer nutrient removals for both transects. Nevertheless, the stations at the Greenwich Meridian transect showed a decrease in the summer removal of nutrients towards the continent. Figure 6d shows the weighted average DFe concentration in the upper layer above the Winter Water – the upper layer from where nutrients are removed. Towards the south less nutrients were removed. In the Weddell Sea, the following trend was observed; removal of nutrients increases northwestwards until ~64.5° S, 44.9° W followed by a sudden drop. For the Weddell Sea, removal of nutrients were consistent with previous findings of Hoppema et al. (2007) for data collected for the same transect in 1993. These authors also observed a sudden decrease in nutrient removal around ~64.5° S. Remarkably, for none of the stations in the Weddell Sea transect a removal of DFe is observed; DFe values are uniform with depth until the Winter Water.

BGD
10, 7433–7489, 2013

4 Discussion

4.1 Comparison with other data in the region

Dissolved Fe data of the open ocean central Weddell Gyre is scarce and mainly available for the surface waters of the near margin region. Here the recently reported DFe data are discussed. Sanudo-Wilhelmy et al. (2002) occupied a transect as far west as 46° W, and reported surface DFe (<1 m depth) concentrations in the range of 0.5–2 nM for off-shelf stations. These reported values are significantly higher than the concentrations reported here, possibly due to the difference in depth; input of atmospheric dust or (surface) ice melt may increase DFe concentrations at the very surface layer. Recently, De Jong et al. (2011) reported DFe data at two stations; first station was an ISPOL station above the slope in the Weddell Sea. The DFe concentration range from 0.6–0.9 nM (upper 200 m) to 1–3 nM (200–1000 m.) and 5–20 nM below 1200 m to bottom (1376vm). These concentrations are significantly higher than the concentrations observed in our transect, particularly in the deep waters. However, the ISPOL station is situated closer to the continent, above the ridge, at ∼1350 m depth and therefore much stronger influenced by bottom sediment resuspension, as also indicated by the lowering of the light transmission signal (De Jong et al., 2011). The other station was situated upstream of the Patagonian continent, on the Scotia Ridge and showed relatively high DFe concentrations (∼3 nM in upper ML; 8–13 nM in 100–750 m depth; 2–4 nM in 1000–3000 m depth and 8–10 nM at 3500 m to bottom (4200 m). This station is situated on the Scotia Ridge and several water masses are observed that have been in contact with the bottom sediments, explaining the higher concentrations of DFe compared to our stations (De Jong et al., 2011). More DFe data in this region is primarily related to sea-ice/iceberg studies. Lannuzel et al. (2008) reported concentrations of 0.9–2 nM in the upper 30 m in the Western Weddell Sea, for a large part as a result of ice-melt. Lin et al. (2011) reported DFe concentrations in the 1–2 nM range for a cruise in the Powell Basin, in March 2009. The relatively higher concentration may be due to the fact that this cruise track was designed to study the effect of icebergs on DFe, and

Discussion Paper | Discussion Paper | Discussion Paper | Discussion Paper |

BGD

10, 7433–7489, 2013

Dissolved Fe across the Weddell Sea and Drake Passage

M. B. Klunder et al.

Title Page
Abstract Introduction
Conclusions References
Tables Figures
◀| |▶
◀ ▶
Back Close
Full Screen / Esc

Printer-friendly Version
Interactive Discussion

therefore may be biased towards area's with high concentrations. Moreover, the Powell Basin is situated downstream of the Peninsula, where shelf derived higher concentrations could be expected. Indeed, the 1–2 nM range is consistent with our stations 222 and 226. In the Drake Passage, Martin et al. (1990) reported surface concentration of 0.16 nM, a minimum of ∼ 0.1 nM at 100 m depth, and increase to 0.4 nM at 500 m depth and Ardelan et al. (2010) reported ∼ 0.2 nM for ACC surface waters and ∼ 1.5–2.5 nM for shelf waters, North of King George Island [data also used in Dulaiova et al. (2009). In an incubation study, Hopkinson et al. (2007) reported concentrations ∼ 0.1–0.14 nM in the open ACC waters to ∼ 1.6–1.7 nM for shelf waters. Our data roughly corresponds to these data, with low concentrations (<0.1 nM) and a DFe minimum at the subsurface in the ACC waters, and DFe concentrations of ∼ 2 nM for shelf waters.

4.2 Distributions of DFe in the Weddell Sea

4.2.1 Surface waters in the Weddell Sea

The very low surface DFe (<LLoD (10 pM) to 100 pM) concentration over most of the Weddell Sea transect indicates a strong (seasonal) depletion of DFe. The significant vertical advection reported for the Weddell Sea (Weppernig et al., 1996; Haine et al., 2008; De Jong et al., 2012) indicates that upwelling from deeper waters is an important source of DFe to the Weddell Sea surface. Moreover, in our study region, melting of floating icebergs (mainly in the Weddell Sea) and sediment derived Fe are important sources, as confirmed by modelling studies (Lancelot et al., 2009) and fieldwork (Dulaiova et al., 2009; Ardelan et al., 2010; Lin et al., 2010). However, this is mainly restricted to the region along the Antarctic Peninsula and less relevant to the Central Weddell Basin (Middag et al., 2012). The Weddell Sea and Scotia Sea are accumulation regions for icebergs (Stuart and Long, 2011) and DFe enrichment due to icebergs is reported (Lin et al., 2011). Lannuzel et al. (2008) reported high (∼ 1 nM) DFe concentrations upon the melting of seasonal sea-ice in the Weddell Sea. However, these concentrations were reported in November–December, at the spring time of sea-ice melt.

BGD
10, 7433–7489, 2013

During our occupation of the transect, in March 2008, any DFe derived from significant sea-ice earlier in the season, would likely already have been taken up by phytoplankton. Possible effect of melting sea-ice or icebergs on the distribution of DFe would be reflected in low salinity. Almost all of the upper 25 m DFe values were <0.1 nM, and salinities were high (>34). However, at station 210 a small enrichment was observed (DFe = 0.16 nM) at 10 m depth corresponding to a slightly lower salinity (33.8) (Figs. 2a, 4a). This could be caused by a small amount of sea-ice meltwater. Deposition of dust is very low in the Weddell Sea and therefore plays a minor role in this region (Duce et al., 1991; Jickells et al, 2001; Cassar et al, 2005). Nevertheless, over time, aerosols may accumulate on sea-ice or on the Antarctic continental Ice Sheet, and deliver (D)Fe to the Weddell Sea water upon melting of this sea-ice.

A significant relationship of dissolved Mn with nutrients (PO_4, NO_3 and Si) and (inverse) with chlorophyll fluorescence indicates biological depletion of Mn from the surface waters of this transect (Middag et al., 2013). No correlation was found for DFe and major nutrients ($R^2 < 0.1$) in the upper 100 m of the Weddell Sea. This may be caused by the complex pattern and seasonality in sources on the one hand and biological uptake and ligand binding and non-biological scavenging of DFe on the other hand. The export of organic carbon and chlorophyll fluorescence are good indicators to discuss the role of (biological) DFe removal during and prior to our cruise. Based on $^{234}Th/^{238}U$ disequilibrium data Rutgers van der Loeff et al. (2011) reported POC export estimates for the same transect and the same cruise. Unfortunately, the POC export data were not always sampled at the same stations as the trace metal data of the Weddell Sea transect. Nevertheless, we can discern the pattern of DFe, biological activity and POC export. Roughly, enough available DFe will increase the biological uptake of DFe (related to fluorescence) and subsequently the POC export. Depending on the time in the season, the DFe pattern may be roughly explained by the pattern of recent biological uptake and less recent uptake, refected by the POC export, reflecting the uptake earlier in time. This is illustrated in Fig. 7, which shows DFe integrated over the upper 100 m, average chlorophyll fluorescence and POC export at 100 m depth (Rutgers van

BGD
10, 7433–7489, 2013

der Loeff et al., 2011). We will use the fluorescence signal from the same cast as the DFe samples as indicator for biological activity at time and place of sampling. We take the good agreement between the average fluorescence over the upper 100 m and the chlorophyll data for the same transect (Neven et al., 2011) ($R^2 = 0.85$; $n = 5$, $p = 0.01$, see Fig. A1) as a confirmation that average fluorescence fairly well represented the phytoplankton abundance. In the eastern part of the Weddell Gyre (~ 17–24° W), the depth-integrated DFe in the upper layer is approximately ~ 8 μmol m^{-2}. Here, recent uptake of DFe was probably low as the fluorescence signal was low. The POC export was somewhat higher compared to other regions. Further west, at ~ 27° W, in the Central Gyre, some higher DFe inventories were observed, despite the increase in chlorophyll a; this could be explained by the low POC export, thus low removal earlier in the season. In contrast, between the stations at ~ 27° W and ~ 36° W, the strong increase in chlorophyll a was also reflected in the strong decrease of the DFe inventory. The lowest DFe surface concentrations were observed where relatively high C export was found, especially at station 204 (~ 43° W). Here, very low integrated DFe (~ 5 μmol m^{-2}) was observed and POC export reached 8.7 mmol m^{-2} d^{-1} (through 100 m depth; Rutgers van der Loeff et al., 2011) (Fig. 7). Moreover, also removal of PO_4, NO_3, Si (not shown) and low Mn (Middag et al., 2013) were observed, indicating biological removal of nutrients and trace metals in the time prior to our cruise. This is confirmed by satellite chlorophyll a data (monthly mean chl-a data; GlobColour Archive) showing an ice edge bloom in this region in February 2008 (Rutgers van der Loeff et al., 2011). Further West, at 48° W, there is and has been an ice cover in the months prior to our cruise, present until the moment of sampling (monthly mean chl *a* satellite data; Rutgers van der Loeff et al., 2011), and very little C export has been observed, which may have allowed higher concentrations of DFe, as well as PO_4, NO_3, Si and Mn (Middag et al., 2012) to be maintained, this likely in combination with recent input due to recent surface ice-melt (see above). Towards the peninsula POC export was high, likely as a result of (another) strong bloom in January 2008 (Rutgers van der Loeff et al., 2011). Uptake from algae in this bloom may have caused some DFe removal, leading to lower concentrations of DFe, despite the closer proximity to the shelf source of Fe (Fig. 4a). Above the shelf, the shelf-derived DFe sources ensure continuously high DFe in this region, although there is large POC export (Rutgers van der Loeff et al., 2011). In this region, little recent biological uptake is expected, because fluorescence data indicates very little phytoplankton abundance in the shelf region (Fig. 7). This is in line with findings of Neven et al. (2011) and satellite derived chlorophyll (Rutgers van der Loeff et al., 2011) and with the relatively strong depletion of nutrients above the shelf.

A continuous input of DFe from the Antarctic shelf region stimulating production and thus nutrient removal in the near margin region, as supposed by Hoppema et al. (2007), would be reflected in the relationship between DFe and the nutrient removal values. However, we did not observe a trend in DFe removal in the Central Weddell Sea. The clarity of the relationship between DFe and the nutrient removal values will decrease depending on the DFe concentrations; if DFe is in major excess, the relationship with nutrient removal may not be identified. Figure 8a–f shows the nutrient removal, amount of depleted nutrients, for both transects relative to the amount of DFe present in the water above the Winter Water layer (weighted average). It is important to note however, that the nutrient removal estimates represent a difference, emerged over spring and summer, whereas DFe value represents the instantaneous DFe concentration at the moment of sampling. It appears that the regions with a strong nutrient removal did indeed have high Fe concentrations, although this was mainly seen in the stations at the Greenwich meridian, which may partially reflect a difference in Fe input between the two regions. Two stations in the west Weddell Sea transect (instead 198 and 204) showed a nutrient removal in accordance with the Greenwich Meridian transect and with earlier findings in this region (Hoppema et al., 2007), despite low DFe concentrations. This may be explained by growth and export of phytoplankton earlier in the season. The depletion of nutrients was observed recently. For DFe, the momentary concentration was probably lower, due to uptake earlier in time, as is consistent with the very high values for POC export observed in the region of station 204. Around station 198, no sample for POC export has been taken, but the fluorescence signal

BGD
10, 7433–7489, 2013

is high (Fig. 7). Likely, concentrations of DFe were high enough to stimulate primary production. The high DFe despite low nutrient removal that is observed in station 210 may be attributed to the recent ice melt (see above), which would not yet have been reflected in the nutrient drawdown. Although the ratio of N:P and N:Si in seawater were also determined by other processes, mainly by continental shelf related processes, at the edge of the transect, the influence of DFe on the N:P and N:Si ratios is visible from these ratios in the seawater. From Fig. A2 it appears that the slightly higher N:P and N:Si ratios (indicating low removal of N relative to P and Si respectively) in the central Gyre at around ~ 35–40° E were consistent with the lowest Fe concentration. At $\sim 48^{\circ}$ W, where higher DFe is observed in the upper 100 m, a decrease

in both nutrient ratios was observed (Fig. A2a and b). This appears to confirm the influence of DFe on the nutrient (uptake)ratios, but mainly in the Central Gyre. Towards both ends of the section, near the Antarctic continent and the Peninsula (Fig. A2a), the ratio of dissolved N:P indeedwas lower.>This is consistent with the higher, more optimal Redfieldian (i.e. towards or at 16:1) uptake ratio by diatoms with a higher ambient DFe concentration. On the other hand, we see a high N:Si dissolved ratio towards the end at the Antarctic side of the transect, which cannot be explained by the remaining nutrients. This station was covered by dense sea-ice at the time of sampling (mid March), and the lower salinity indicates an influence of meltwater in this region. However, the months before the occupation of the station it has been ice-free [Heygster et al., 2012]. Chemical processes related to forming and melting of sea-ice (brine formation, brine release and nutrient uptake by the under-ice phytoplankton community) strongly affect sea ice and surrounding water nutrient concentrations (Vancoppenolle et al., 2010). At this station, a lower nitrate as well as in silicate concentration was observed compared to the rest of the transect. However, the drop in silicate is much stronger than that in nitrate, as well relative as absolute. A very low value of both nutrients in the ice meltwater would stronger influence the silicate concentration compared to nitrate, thus increase the N:Si ratio. Although the study was performed in December, indeed in Weddell Sea sea-ice, a very low amount of nutrients is observed (Lannuzel

BGD
10, 7433–7489, 2013
Dissolved Fe across the Weddell Sea and Drake Passage
M. B. Klunder et al.

et al., 2008). However, no final conclusions can be drawn about the increase in N/Si ratio at station 187, as no data from the sea-ice in this region is available.

Diatoms are the most abundant phytoplankton species in the Weddell Sea. For blooms of the diatom Fragilariopsis kerguelensis at the Polar Front, it has been shown that uptake of nitrate can be severely impaired under Fe-limiting conditions (De Baar et al., 1997, overview in Marchetti and Cassar, 2009). Briefly, Fe is essential in the enzymes nitrate reductase and nitrite reductase for reductive conversion of nitrate into ammonia for synthesis of amino acids of proteins (Geider and La Roche, 1994; De Baar et al., 1997). Under Fe-stress, this conversion is hampered, while the uptake and incorporation of phosphate and silicate is not directly affected. As a result the biomass of Fe-limited diatoms has anomalously low N:P and N:Si element ratios while on the other hand the seawater left behind shows anomalously high N:P ratios (De Baar et al., 1997) and N:Si ratios (Takeda et al., 1998). Figure 8d shows the estimated nutrient removal relative to the weighted average DFe, and generally shows the lowest (<0.4) N:Si removal ratio at lower DFe (<0.1 nM) concentrations and the highest N:Si removal ratios (>0.4) at DFe >0.1 nM concentrations. The diatom Fragilariopsis kerguelensis and other major bloomforming Antarctic diatoms are heavily silicified and a ratio N:Si = ~0.4 is normal under Fe replete conditions (De Baar et al., 1997).

Regarding P:Si (Fig. 8e) and N:P (Fig. 8f) removal ratios, the results were not so straightforward. There is a tendency of increasing N:P removal ratio (from ~5 to ~15) with increasing DFe, but this is only visible for the Greenwich meridian stations. The Weddell Sea stations showed a relatively constant N:P removal ratio (~13) with DFe. In general, this removal of the nutrient ratios wass consistent with the ratios of the remaining nutrients in the seawater; the higher N:Si removal ratio (0.8) was found at station 210 (48.278° W)(Fig. 8d), where a lower N:Si ratio in the seawaterwass observed (Fig. A2a). The somewhat higher removal ratio at station 187 (17.947° W) cannot be explained by the remaining nutrients, and is likely explained by the sea-ice coverage and related nutrient dynamics of the melting and formation of sea-ice (Vancoppenolle et al., 2010) from the months before the cruise until the time of sampling. It is possible

BGD
10, 7433–7489, 2013

Dissolved Fe across the Weddell Sea and Drake Passage

M. B. Klunder et al.

that the nutrient ratio observed at the day of actual sampling does not fully reflect the removal ratio in the preceding months, explaining the differences in preceding summertime N:P removal and N:P ratio at the moment of sampling. For N:P removal, the higher ratio (20.5) observed at station 187, is consistent with a lower N:P ratio remaining in the seawater (Fig. A2b). Unfortunately, a comparison between the depletion and the remaining nutrients close to the shelf is not possible, because the Winter Water was not observed west of 48.278° W at the Weddell Sea transect (see Sect. 2)The difference in N:P removal ratio between the two regions could be explained by a upwelling of waters from below with different nutrient signature (such as NADW with a relatively high N:P (De Baar et al., 1997)). To test this hypothesis, the surface (0–150 m) concentrations of major nutrients (N,P,Si) were subtracted from the subsurface (150–250 m) and intermediate (250–1000 m) nutrient concentrations; no differences were observed between the regions. Thus this hypothesis can be discarded.

The difference in nutrient uptake ratios might then be explained by a different species composition. Both regions are dominated by diatoms (Alderkamp et al., 2010); however, in the Central Weddell Sea stations the size of the diatoms is generally somewhat smaller (Neven et al., 2011). From the same expedition, specific counts and measurements of the phytoplankton community are available for stations at the Greenwich meridian (150, 161, 167 and 178) and for stations in the Eastern Weddell Gyre (191, 193, 198, 204 and 210), see Fig. 1a. Here we use estimations of the size of the diatoms present in both regions. On average diatoms were significantly smaller in terms of biovolume (T-test, $p<0.1$) in the Eastern Weddell Sea region (average 4258 ± 1883 mum^3) than at the Greenwich Meridian (average 6981 ± 2397 mum^3) (Table 1). Moreover, there is a larger number of smaller (<1000 mum^3) diatoms in the Eastern Weddell region compared to the Greenwich Meridian (7 % and 3 % respectively) and the lower number of large diatoms (>5000 mum^3) (70 % and 84 % respectively (Table 1). Marchetti and Cassar (2009) summarized several studies of the effect of iron deficiency on nutrient uptake and reported stronger Si relative to N uptake in Fe limited diatoms, dependent on diatom size. There are two mechanisms via which the

BGD
10, 7433–7489, 2013

N:P uptake ratio of diatoms is influenced by their size. First, the specific growth rate of diatoms with regard to Fe is dependent on their surface to volume (S/V) ratio (Sarthou et al,2005; De Baar et al., 2005); smaller diatoms generally have a larger S/V ratio which is beneficial in their Fe uptake (see also Timmermans et al., 2004). This benefit is because a larger S/V ratio allows more uptake relative to the intracellular needs, but also because smaller cells have a smaller diffusive boundary layer thickness, which lowers the concentration gradients (Marchetti and Cassar, 2009). Therefore, impairment of N uptake as a result of Fe limitation (De Baar et al., 1997) is more likely to occur in larger species, as observed in the Greenwich Meridian stations. Also the uptake kinetics of nitrogen depends on the S/V ratio, whereas such a relation is not found for P uptake (Sarthou et al., 2005). Our findings for the N:P removal ratios are in line with culture experiments of Timmermans et al. (2004). They reported that the largest species (small S/V ratio) showed the strongest effect of Fe depletion in their N:P uptake; and this effect became less with smaller species. The fact that larger species take up N less efficiently relative to P could contribute to the low N:P removal ratios found at low DFe in the Greenwhich Meridian stations, while these are not found at similar DFe in the Central Weddell Sea.

During the EIFEX in situ iron fertilization experiment, Hoffmann et al. (2006) found for the large (>20 µm) size class of phytoplankton, comprising large diatoms, that at low ambient dissolved Fe this large size class had cellular N:P ratio of ∼ 5, which upon DFe enrichment increased to ∼ 15–16. Such differences were absent for the smaller (<20 µm) size classes. These diatom size classes are comparable to the median size of diatoms of 20–25 µm observed in our study. We conclude that the low N:Si and N:P uptake ratios indicate the important, and possibly limiting, role of DFe for phytoplankton abundance and for the uptake and cycling of nutrients in the Weddell Sea. However, many other factors are involved, amongst which are species composition and size. Finally please notice here that the DFe concentrations in the surface waters along the transect are low (<0.25 nM) compared to the concentrations in the enrichment treatments of the experiments mentioned above (Takeda, 1998; Timmermans et al., 2001

BGD
10, 7433–7489, 2013

and Hoffmann et al., 2006) and therefore the relative effects of DFe availability are expected to be lower in our field situation compared to the abovementioned studies.

4.2.2 Deep waters in the Weddell Sea

In the deep waters in the Weddell Sea the dissolved Fe concentrations are very low, and gradually increase with depth. Following the properties derived by Klatt et al. (2005) (See Sect. 3), can calculate the DFe in the different water masses in the Weddell Sea; in the WDW the concentration was 0.21 ± 0.08 ($n = 52$), in the WSDW was 0.32 ± 0.12 ($n = 42$) and in the WSBW was 0.35 ± 0.10 ($n = 11$). For comparison, Klunder et al. (2011) reported concentrations of deep waters of the Weddell Gyre at the Greenwich meridian; a DFe concentration of 0.3 ± 0.14 nM in deep waters (WDW, WSDW, WSBW) in the westward flowing southernmost limb of the Weddell Gyre, and 0.47 nM $\pm$ 0.16 nM in the, more northern, eastward flowing limb. As expected, the concentrations here observed are similar, but slightly lower than those observed in the westward flowing component at the Greenwich Meridian. This is the same water mass, and apparently some DFe was lost due to scavenging removal during transit from 0° W to the Weddell Sea. However, there was a large difference in DFe concentration between the Weddell Sea transect deep waters and the eastward limb of the Weddell Gyre at the Greenwich Meridian. This indicates that on its way eastwards, there must be significant input of DFe to the deep waters at the South Scotia Ridge. These sources could be either sediment resuspension or DFe flux from the sediment at the South Scotia Ridge ridge and/or inflow of Circumpolar Deep Waters in the 45–55° S region as observed by Matano et al. (2002). Also hydrothermal input from the South Scotia Ridge is an important Fe input source (Klinkhammer et al., 2001). Moreover, there are indications of iron input close to the Greenwich Meridian, at the Scotia Ridge (Klunder et al., 2011). The DFe concentrations in this part of the Greenwich Meridian will not only be influenced by the Weddell Gyre but also by inflow of CDW from the North and deeper waters from the South (Klunder et al., 2011)

BGD
10, 7433–7489, 2013

The deep water masses leave the Weddell Sea and form the AABW flowing into the ACC and the abyssal world oceans (Naviera Garabato et al., 2002; Hoppema et al., 2010). The here reported DFe concentrations of ~0.32 ± 0.12 nM for WSDW and 0.35 ± 0.10 nM for the WSBW, thus eventually for the AABW, are on the lower end of the wide range of DFe concentrations observed in AABW throughout the Atlantic Ocean; ~0.3 nM (Klunder et al., 2011), 0.38–0.8 nM Chever et al., 2010) and 0.28-0.93 nM (Rijkenberg et al., 2011 abstracts Liege and Goldschmidt Prague) for the South Atlantic and 0.7–0.8 nM (Laës et al., 2003), 0.7 nM (Thuroczy et al., 2010, ~0.36–0.92 nM) (Rijkenberg et al., 2011a and b) for the North Atlantic. This suggests DFe enrichment of AABW, likely by mixing with overlying NADW as well as supply from underlying sediment on its way northwards.

Downslope convection of surface waters close to the Peninsula, along the slope, renewing WSBW has been observed in the Weddell Sea. This was also seen in the θ sections of our cruise (Fig. 3). Moreover, recently observed maxima in dissolved barium (Hoppema et al., 2010), iodate , CFC-12 (Bluhm et al., 2011), DAl and DMn (Middag et al., 2013) in the WSBW, indicate such downslope movement of dense shelf waters. The distribution of DFe is not conclusive regarding this downslope convection of WSBW; little enrichment was observed at ~51° W, 2500 m depth, despite indications of shelf water input (low θ (not shown) and higher DMn (Middag et al., in press)). However, in the deeper waters, some enrichment of DFe was observed, corresponding to lower θ, thus indicating DFe enrichment of WSBW due to downslope convection. Unlike for dissolved Ba (Hoppema et al., 2010) , the DFe delivered by this process to the WSBW appears to be not sufficient to significantly enhance the DFe concentration in the overlying WSDW by subsequent upward mixing supply.

BGD
10, 7433–7489, 2013

4.3 Distributions of Fe in Drake Passage

4.3.1 Surface and sub-surface waters in Drake Passage

During our cruise, we observed an input of DFe from the shelves around Elephant Island into the Drake Passage, consistent with earlier findings of DFe (e.g. (Dulaiova et al., 2009), DMn and DAl concentrations from the same stations (Fig. 9; Middag et al., 2012)). Above the shelf, high DFe concentrations were observed at the σ_θ isopycnal levels of 27.5 (1.87 nM), 27.55 (1.5 nM) and ∼ 27.64 (1.8 nM). The first two peaks were observed at station 230, but not as seperate peaks, but rather as a broad peak. Unfortunately there were no samples at this σ_θ level at station 236 (Fig. 9). Remarkably, the peak at σ_θ 27.64 was observed as a small peak at station 220 but not further offshore at station 230. This illustrates the many dynamic small gyre like structures observed to the north of Elephant Island (Ardelan et al., 2010 (their figure 10); Hewes et al., 2009) causing a complex pattern of off-shelf currents in this region. The input of DFe from the Antarctic Peninsula shelf north of Elephant Island is in line with findings from Ardelan et al. (2010), who observed DFe enrichment at σ_θ = 27.5–27.6. Moreover, Charette et al. (2011) reports maximum concentration of radium (Ra) values at σ_θ = 27.5–27.6 for this region, indicating shelf-derived waters. Despite the low number of stations, we estimated the scale length (distance where the DFe concentration is 1/e of the initial concentration) at ∼ 200 km. This is reasonably similar to the scale length for DFe observed for shelf input in the Nansen Basin (Arctic Ocean) (∼ 263 km). As in the Drake Passage (Renault et al., 2011), also in the Nansen Basin the direction of the shelf current is perpendicular to the shelf (Klunder et al., 2011) resulting in a relatively short scale length as compared to other regions (Johnson et al., 1997). In our study region, Nielsdottir et al. (2012) reported a scale length in the same order, ∼ 102 km, for transects at South Georgia island and Bird Island. The scale length of ∼ 200 km is considerably higher than the ∼ 25 km reported by Ardelan et al. (2010) for the same region. This may partially be explained by the fact that latter scale length is calculated for the upper ∼ 50 m, not for the subsurface maximum, and would indicate more rapid

BGD
10, 7433–7489, 2013

removal of Fe from the upper 50 m compared to the subsurface maximum, most likely due to biological uptake.

Further into the Drake Passage, at ~350 km from the shelf, the shelf waters carrying a visible DFe signal are found in the subsurface, below a low DFe upper layer of 150 m. In the North part of the Drake Passage, this low DFe layer extended to ~500 m depth (Fig. 2b). The DFe = 0.2 nM contour approximately coincided with the 34.2 isohaline and with the surface and subsurface water masses (SASW, AASW and WW) as classified by Sudre et al (2011) for this transect. Maximum primary production in the Drake Passage is observed in the December–February period (Moore and Abbott (2001. Biological removal of DFe from the surface waters and subsequent downwards transport may cause the sharp difference in DFe concentrations between these surface waters and the deeper Circumpolar Deep Waters (Fig. 5a). Moreover, given the strong geostrophic velocities for the surface waters of our transect (0.1–0.4 $m\,s^{-1}$ at 100 m depth; (Renault et al., 2011)) these (sub)surface waters originate (mostly) from the South Pacific Ocean, providing an additional explanation for the low DFe concentrations at the surface. These waters from the Pacific Sector of the Southern Ocean were low in DFe (~0.05 nM in the 100–120° W region in January/February (Gerringa et al., 2012) and ~0.2 nM at 120° W in March/April (De Baar et al., 1999)), due to biological removal or lack of input sources (De Baar et al., 1999; Hiscock et al., 2001).

An exception to the generally low concentration of DFe is the relatively high DFe concentration observed in the uppermost water column at station 238. A concentration of 1.32 nM and 0.29 nM at 10 and 25 m depth respectively is followed by DFe depleted waters (<0.06 nM) in the upper 200 m. This surface maximum shows good correspondence with high dissolved Al concentrations at the same depths (Middag et al., 2012). Five day NOAA HYSPLIT backwards trajectory (Fig. A3) confirm that the air above this region originates from Patagonia. The nearby station 241 did not show an upper surface maximum despite air originating from Patagonia, which may be explained by lack of shipboard precipitation (rain). Data shows that in the 24 hours prior to occupation of station 238 there had been significant precipitation, whereas during the hours before

BGD
10, 7433–7489, 2013

occupation of station 241 no precipitation is reported (supplementary table S2). Wet deposition by precipitation in commonly lower pH rainwater (as compared to high pH ∼ 8.1 of seawater) is deemed to strongly enhance dissolution of dust, relative to dry deposition (Jickells and Spokes, (2001); De Baar and De Jong, (2001))

The 400 m deep station above the Patagonian shelf, close to Tierra del Fuego, showed high dissolved Fe concentrations in the upper 150m, where salinity was low (Figs. 2b, 5a). There was a strong inverse correlation between DFe and salinity (R^2 =0.85, $P<0.001$, n=11), pointing towards fluvial input of DFe. Similar high concentrations and correlations were observed for DMn and DAl (Middag et al., 2012). This DFe maximum is only observed in the most northern station, above the shelf (Fig. 5a), but does not extend far into the Drake Passage. The latter may be explained by the very strong eastward velocity in this region (>40 cm/s; (Renault et al., 2011) bringing the elevated Fe signal more eastward than the other stations of our section. Although the amount of freshwater flowing into the Drake Passage is relatively small, the order of magnitude higher DFe in these waters compared to the common Drake Passage surface waters, may cause substantial DFe enrichment of the surface waters to the East.

4.3.2 Deep waters of Drake Passage

In the Southern Drake Passage, around 59–60° S, a strong enrichment in DFe was observed in the bottom waters (>3000m) (Fig. 5a). This enrichment was also observed in the concentrations of DMn and DAl (Middag et al., 2012). These enrichments could be caused by downslope convection of dense water along the slope. Meredith et al. (2003) reported a direct ventilation of deep waters in the Drake Passage by dense shelf waters north of Elephant Island. This mechanism was only observed during and after austral winter, and was strongest in ENSO years, although 2008 had a strong negative ENSO index (Jullion et al., 2010). Moreover, Sudre et al. (2011) have shown that WSDW may follow a westward direction upon leaving the Weddell Sea through the gaps in the South Scotia Ridge. Huhn et al. (2008) reported a similar pathway for WSBW formed along

BGD
10, 7433–7489, 2013

the Peninsula Slope in the Western Weddell Sea. Concentrations of DFe in the deep waters in the Southern Drake Passage are significantly higher than those in the WSDW and WSBW in the Weddell Sea (Fig. 2); parallel with higher DMn and DAl (Middag et al., 2012)). Thus there is likely a source of trace elements during transport from the Weddell Sea to Drake Passage. Although hydrothermal vents are present in this region (Klinkhammer et al., 2001), DFe enrichment by mixing with hydrothermally influenced waters is unlikely, because this would be reflected in enhanced δ^3He concentrations, which are not observed (Sudre et al., 2011). The lowered light transmission (Middag et al., 2012) in these water masses is an indication of resuspended particles, likely picked up during transport from the Weddell Sea to the Drake Passage. Dissolution of these particles or mixing with DFe rich pore waters during this resuspension might be the reason for the observed high DFe concentrations. This mechanism has also been suggested for DMn and DAl by Middag et al. (2012).

In terms of DFe, the circumpolar Deep Waters were enriched relative to the SPDW observed below and AAIW observed above. From 2000–3000 m depth ascending southwards, the Circumpolar Deep Waters (LCDW/UCDW) bring slightly more DFe (>0.5 nM) to the surface waters, in the Southernmost part of the transect. Above the UCDW, relatively low DFe waters >0.25 nM were transported northwards as AAIW. However, these waters do not reach deeper than 500 m, as there was a water layer with high DFe at 55.5–57° S from 500–1000 m.

A layer with an anomalously high DFe concentration (up to 1.94 nM) was observed towards the South American flank of the Drake Passage, at ~2000–3000 m depth. This relatively small water mass has earlier been classified by Well et al. (2003) and Sudre et al. (submitted) as South Pacific Deep Slope Water, originating from the East Pacific Rise (EPR), carrying a significant δ^3He signal as a result of the hydrothermal activity at the EPR (Well et al., 2003). Middag et al. (2012) reported a clear trend between δ^3He and DMn, both good indicators for hydrothermal vents, in this water mass. We assume the high concentrations of DFe in the SPDSW water are also caused by hydrothermal activity. Although the volume of this water mass is small, the large

BGD
10, 7433–7489, 2013
Dissolved Fe across the Weddell Sea and Drake Passage
M. B. Klunder et al.

difference in DFe (1.5–2 nM) relative to its surrounding deep water masses (~ 0.5 nM) results in the SPDSW being a considerable source of DFe to the deep waters in the Drake Passage, and eventually to the deep South Atlantic Ocean.

5 Summary and conclusions

Surface dissolved Fe concentrations can reach very low values (~ 0.01 nM) in the Central Weddell Sea. Generally, concentrations are <0.1 nM in the upper 100 m. These low DFe concentrations in the upper 100 m can be (partly) explained by primary productivity in the surface waters, stressing the important role of biological processes in the DFe distribution. The only DFe input from the Antarctic Peninsula shelf is observed above the shelf, with little sign of advection of these waters into the Weddell Basin. Dissolved Fe in the deep water masses of the Weddell Sea is low compared to that north of the Weddell Basin, and also to deep water concentrations observed worldwide (Moore and Braucher, 2008). In the Weddell Sea, no clear influence of the shelf is observed in the seasonal nutrient or DFe drawdown, although it should be noted that no Winter Water was observed north of 64° S, and thus no removal values could be reported close to the shelf. The Si:N removal ratio is greater in low DFe regions indicating DFe control on the algal nutrient uptake ratios and eventually on algal growth. In the Eastern Weddell Gyre, no effect of DFe on the N:P removal ratio (~ 13) was observed. At the Greenwich Meridian, however, the N:P removal ratio increased with increasing DFe. This difference between regions is likely caused by differences in diatom size; the diatoms at the Greenwich meridian are significantly larger. Our results indicate that DFe enrichments due to shelf sources are restricted to the Antarctic Peninsula shelf, and do not have a large scale effect on the DFe concentration and on the related nutrient removal in the Weddell Gyre. Nevertheless, the concentration of DFe appears to influence diatom growth in the Weddell Sea, although this effect is dependent on diatom size. The difference in deep water DFe concentrations between the transect here presented and the 0° W transect indicates significant enrichment of deep waters with DFe

Discussion Paper | Discussion Paper | Discussion Paper | Discussion Paper |

BGD

10, 7433–7489, 2013

Dissolved Fe across the Weddell Sea and Drake Passage

M. B. Klunder et al.

during eastward transit along the Scotia Ridge. There is an indication of some DFe enrichment with formation of WSBW by downslope convection of shelf waters. However, the small difference in DFe between WSBW and WSDW suggests that this is not a significant DFe source to the WSDW. In the Drake Passage, close to Elephant Island, strong (~ 2 nM) DFe input from the shelf is observed, following the same isopycnals as earlier observed for shelf water input in this region. The scale length of ~ 200 km indicates that DFe enrichment does extend into the Drake Passage. Moreover, the strong eastward velocities of the ACC, turn the shelf region into a source of DFe for regions further East, thus supporting the more intense summer plankton blooms in the Scotia Sea (Borrione and Schlitzer, 2010). Generally, surface waters in the Drake Passage have low DFe concentrations (<0.2 nM), as a result of biological removal, both in Drake Passage and further west, in the remote South Pacific, where DFe concentrations are very low in surface waters. Locally, DFe enrichment is observed caused by atmospheric (58.3° S) or fluvial input sources (55.1° S; above Patagonian shelf). Dissolved Fe concentrations of >1 nM are observed in the deep waters in the South of the Drake Passage, likely coming from Weddell Sea Deep Waters, enriched with DFe by sediment and porewater resuspension or a flux from the porewaters during transit over the Scotia Ridge. Further into the Drake Passage, the distribution of DFe generally follows the water masses, with highest DFe in the Circumpolar Deep Waters. Towards the shelf of Tierra del Fuego, strong DFe enrichment is observed in the South Pacific Deep Slope Water, a water mass coming from the Pacific carrying hydrothermal properties, notably elevated Mn and δ^3He (Middag et al., 2012 and Sudre et al., 2011).

Supplementary material related to this article is available online at: http://www.biogeosciences-discuss.net/10/7433/2013/ bgd-10-7433-2013-supplement..zip.

BGD
10, 7433–7489, 2013

Acknowledgements. The authors are most grateful to the master and crew of FS Polarstern for their excellent support and commitment during ANT XXIV-3. We would like to thank M. Rijkenberg and P.Sedwick for useful comments. We would also like to thank Sven Ober and Gerd Rohardt from the Alfred Wegener Institute for provding the physical parameters. We commemorate our colleague Willem Polman who unfortunately did not return from ANT XXIV-3.

References

Alderkamp, A.-C., de Baar, H. J. W., Visser, R. J. W., and Arrigo, K. R.: Can photo inhibition control phytoplankton abundance in deeply mixed water columns of the Southern Ocean?, Limnol. Oceanogr., 55, 1248–1264, doi:10.4319/lo.2010.55.3.1248, 2010.

Alderkamp, A.-C., Garcon, V., De Baar, H. J. W., and Arrigo, K. R.: Short-term photoacclimation effects on photoinhibition of phytoplankton in the Drake Passage (Southern Ocean), Deep Sea Res. Pt. I, 58, 943–955, 2011.

Ardelan, M. V., Holm-Hansen, O., Hewes, C. D., Reiss, C. S., Silva, N. S., Dulaiova, H., Steinnes, E., and Sakshaug, E.: Natural iron enrichment around the Antarctic Peninsula in the Southern Ocean, Biogeosciences, 7, 11–25, doi:10.5194/bg-7-11-2010, 2010.

Baars, O. , Croot, P. : The speciation of dissolved zinc in the Atlantic Sector of the Southern Ocean, Deep-Sea Res. Pt. II, 58, 2720–273, 2011.

Bluhm, K., Croot P., Huhn O., Rohardt G., and Lochte K. :Distribution of Iodide and iodate in the Atlantic sector of the southern ocean during austral summer, Deep-Sea Res. Pt. II, 58, 2733–2748, 2011.

Blain et al.: Effect of natural iron fertilization on carbon sequestration in the Southern Ocean, Nature, 44, doi:10.1038/nature05700, 2011.

Borrione, I. and Schlitzer, R.: Aqua MODIS satellite measurements over the Scotia Sea: spatial and temporal variability of phytoplankton blooms, 2010 Ocean Sciences Meeting, 2010.

Boyd, P. W., Jickells, T., Law, C. S., Blain, S., Boyle, E. A., Buesseler, K. O., Coale, K. H., Cullen, J. J., De Baar, H.J.W., Follows, M., Harvey, M., Lancelot, C., Levasseur, M., Owens, N. J. P., Pollard, R., Rivkin, R. B., Sarmiento, J., Schoemann, V., Smetacek, V., Takeda, V.,Tsuda, A., Turner, S., and Watson, A: Mesoscale iron enrichment experiments 1993–2005: synthesis and future directions, Science, 315, 612–617, 2007.

Bucciarelli, E., Blain, S., and Tréguer, S.: Iron and manganese in the wake of the Kerguelen Islands Southern Ocean, Mar. Chem., 73, 21–36, 2001.
Buma, A. G. J., De Baar, H. J. W., Nolting, A. J., and van Bennekom, R. F.: Metal enrichment experiments in the Weddell-Scotia Seas: Effects of iron and manganese on various plankton communities, Limnol. Oceanogr., 36, 1865–1878, 1991.
Cassar, N., Bender, M. L., Barnett, B. A., Fan, S., Moxim, W. J., Levy II, H., and Tilbrook, B.: The Southern Ocean biological response to aeolian iron deposition, Science 317, 1067–1070, 2007
Charrette , M.: The Role of Ocean Mixing in Southern Ocean Iron-fueled Phytoplankton Blooms: Insight from Radium Isotopes, Presentation at the The Modeling and Synthesis of Southern Ocean Natural Iron Fertilization Workshop, Woods Hole, Monday June 27, 2011.
Chever, F., Bucciarelli, E., Sarthou, G., Blain, S., and Bowie, A. R.: An iron budget during the natural iron fertilization experiment KEOPS (Kerguelen Islands, Southern Ocean), Biogeosciences, 7, 455–468, 2010, http://www.biogeosciences.net/7/455/2010/.
Chever, F., Bucciarelli, E., Sarthou, G., Speich, S., Arhan, M., Penven, P., and Tagliabue, A: Physical speciation of iron in the Atlantic sector of the Southern Ocean along a transect from the subtropical domain to the Weddell Sea Gyre, J. Geophys. Res., 115, C10059, doi:10.1029/2009JC005880, 2010.
Croot, P. L., Andersson, K., Öztürk, M., and Turner, D. R.: The distribution and speciation of iron along 6° E in the Southern Ocean, Deep Sea Res. Pt. II, 51, 2857–2879, 2004.
Croot., P. Baars, O., and Streu, P.: The distribution of dissolved zinc in the Atlantic Sector of the Southern Ocean, Deep-Sea Res. Pt. II, 58, 2707–2719, 2011.
De Baar, H. J. W., Buma, A. G. J., Nolting, R. F., Cadée, G. C., Jacques, G., and Tréguer, P. J.: On iron limitation of the Southern Ocean: experimental observations in the Weddell and Scotia Seas, Mar. Ecol. Prog. Ser., 65, 105–122, 1990.
De Baar, H. J. W., De Jong, J. T. M., Bakker, D. C. E., Löscher, B., Veth, C., Bathman, U., and Smetacek, V.: Importance of iron for plankton blooms and carbondioxide drawdown in the Southern Ocean, Nature, 373, 412–415, 1995.
De Baar, H. J. W., van Leeuwe, M. A., Scharek, R., Goeyens, L., Bakker, K. M. J., and Fritsche, P.: Nutrient anomalies in Fragilariopsis Kerguelensis blooms, iron deficiency and the nitrate/phosphate ratio (A.C. Redfield) of the Antarctic Ocean, Deep Sea Res. Pt. II, 44, 229–260, 1997.

BGD
10, 7433–7489, 2013

Dissolved Fe across the Weddell Sea and Drake Passage

M. B. Klunder et al.

De Baar, H. J. W., de Jong, J. T. M., Nolting, R. F, Timmermans, K. R., van Leeuwe, M. A., Bathmann, U., Rutgers van der Loeff, M., and Sildam, J.: Low dissolved Fe and the absence of diatom blooms in the remote South Pacific Ocean, Mar. Chem., 66, 1–34, 1999.
De Baar, H. J. W. and de Jong, J. T. M.: Distributions, sources and sinks of iron in seawater, in: Biogeochemistry of Iron in Seawater edited by: Turner, D. and Hunter, K. A., IUPAC Book Series on Analytical and Physical Chemistry of Environmental Systems, 7(Chapter 5), 123–254, 2001.
De Baar, H. J. W., Boyd, P. W. , Coale, K. H., Landry, M. R., Tsuda, A., Assmy, P., Bakker, D. C. E., Bozec, Y., Barber, R. A., Brzezinski, M. A., Buesseler, K. O., Boyé, M., Croot, P. L., Gervais, F., Gorbunov, M. Y., Harrison, P. J., Hiscock, W. T., Laan, W. T., Lancelot, C., Law, C., Levasseur, M., Marchetti, A., Millero, F. J., Nishioka, J., Nojiri, Y, Oijen, T. v., Riebesell, U., Rijkenberg, M. J. A, Saito, H., Takeda, S., Timmermans, K. R., Veldhuis, M. J. W., Waite, A., and Wong, C. S.: Synthesis of Iron Fertilization Experiments: From the Iron Age in the Age of Enlightenment, in: The Oceans in a High-CO_2 World, edited by: Orr, J. C., Pantoja, S., and Pörtner, H.-O., J. Geophys. Res.-Oceans, 110, 1–24, 2005.
Duce, R. A. and Tindale, N. W.: Atmospheric transport of iron and its deposition in the ocean, Limnol. Oceanogr., 36, 1715–1726, 1991.
Dulaiova, H., Ardelan, M. V., Henderson, P. B., and Charette M. A.: Shelf-derived iron inputs drive biological productivity in the southern Drake Passage, Global Biogeochem. Cy., 23, doi:10.1029/2008GB003406, 2009.
Elrod, V. A., Berelson, W. M., Coale, K. H., and Johnson, K. S.: The flux of iron from continental shelf sediments: amissing source for global budgets, Geophys. Res. Lett., 31, doi:10.1029/2004GL020216, 2004.
Fahrbach, E., Rohardt, G., Schroder, M., and Strass, V.: Transport and structure of the Weddell Gyre, Ann. Geophys., 12, 840–855, 1994, http://www.ann-geophys.net/12/840/1994/.
Geider, R. J. and La Roche, J.: The role of iron in phytoplankton photosynthesis, and the potential for iron-limitation of primary productivity in the sea, Photosyt. Res., 39 , 275–301, 1994.
Gerringa, L. J. A., Alderkamp, A. C., Laan, P., Thuróczy, C.-E., De Baar, C.-E., Mills, M. M., van Dijken, G. L., Haren, H., and VanArrigo, K. R.: Fe from melting glacier fuels the algal bloom in Pine Island Bay (Amundsen Sea, Southern Ocean), Deep-Sea Res. Pt. II, 71–76, 16–31, 2012.

BGD
10, 7433–7489, 2013

bibitem1 Haine, T. W. N., Watson, A. J., Liddicoat, M. I., and Dickson, R. R., The flow of Antarctic Bottom Water the Southwestern Indian Ocean estimated using CFC's, J. Geophys. Res., 103, 27637–27653, 1998.
Hewes, C. D., Reiss, C. S., and Holm-ansen, O.: A quantitative analysis of sources for summertime phytoplankton variability over 18 years in the South Shetland Islands (Antarctica) region, Deep Sea Res. Pt. I., 56, 1230–1241, 2009.
Heygster, G., Melsheimer, C., and Notholt, J.: Institute of Environmental Physics, University of Bremen, Germany, Sept. 2007, AMSR images: http://iup.physik.uni-bremen.de, Sep. 2011.
Hiscock, M. R., Marra, J., Smith Jr., W. O., Goericke, R., Measures, C., Vink, S., Olson, R. J., Sosik, H. M., and Barber, R. T.: Primary productivity and its regulation in the Pacific Sector of the Southern Ocean. Deep-Sea Res. Pt. II, 50, 533–558, 2003.
Hoffman, L. J., Peeken, I., Lochte, K., Assmy, P., and Veldhuis, M.: Different reactions of Southern Ocean phytoplankton size classes to iron fertilization, Limnol. Oceanogr., 51, 1217–1229, 2006.
Hopkinson, B. M., Mitchell, G., Reynolds, R. A., Wang, H., Selph, K. E., Measures, C. I., Hewes, C. D., Holm-Hansen, O., and Barbeau, K. A.: Iron limitation across chlorophyll gradients in the southern Drake Passage: Phytoplankton responses to iron addition and photosynthetic indicators of iron stress, Limnol. Oceanogr., 52, 2540–2554, 2007.
Hoppema, M., De Baar, H. J. W., Fahrbach, E., Hellmer, H., and Klein, B., Substantial advective iron loss diminishes phytoplankton production in the Antarctic Zone, Global Biogeochem. Cy., 17, 1–9, 2003.
Hoppema, M., Middag, R., De Baar, H. J. W., Fahrbach, E., van Weerlee, E. M., and Thomas, H.: Whole season net community production in the Weddell Sea, Polar Biol., 31, 101–111, 2007.
Hoppema, M., Dehairs, F., Navez, J., Monnin, C., Jeandel, C., Fahrbach, E., and De Baar, H. J. W.: Distribution of barium in the Weddell Gyre: Impact of circulation and biogeochemical processes, Mar. Chem., 122, 118–129, 2010.
Huhn, O., Hellmer, H. H., Rhein, M., Rodehacke, C., Roether, W., Schodlok, M. P., and Schröder, M.: Evidence of deep- and bottom-water formation in the western Weddell Sea, Deep-Sea Res. Pt. II, 55, 1098–1116, 2008.
Jickells, T. D. and Spokes, L. J.: Atmospheric iron inputs to the oceans, in: Biogeochemistry of Iron in Seawater, edited by: Turner, D. and Hunter, K. A., IUPAC Book Series on Analytical and Physical Chemistry of Environmental Systems, Vol. 7, 123–254 (Chapter4), 2001.

BGD
10, 7433–7489, 2013

Jullion, L., Jones, S. C., Naveira Garabato, A. C., and Meredith, M. P.: Wind controlled export of Antarctic Bottom Water from the Weddell Sea, Geophys. Res. Lett., 37, doi:10.1029/2010GL042822, 2010.
Kahru, M., Mitchell, B. G., Gille, S. T., Hewes, C. D., and Holm-Hansen, O., Eddies enhance biological production in the Weddell-Scotia Confluence of the Southern Ocean, Geophys. Res. Lett., 34, doi:10.1029/2007GL030430, 2007.
Klatt, O., Fahrbach, E., Hoppema, M., and Rohardt, G.: The transport of the Weddell Gyre across the Prime Meridian, Deep Sea Res. Pt. II, 52, 513–528, 2005.
Klinkhammer, G. P., Chin, C. S., Keller, R. A., Dählman, A., Sahling, H., Sarthou, G., Petersen, S., Smith, F., and Wilson, C.: Discovery of new hydrothermal vent sites in Bransfield Strait, Antarctica, Earth Planet. Sci. Lett., 193, 395–407, 2001.
Klunder, M. B., Laan, P., Middag, R., de Baar, H. J. W., and van Ooijen, J. C.: Dissolved Fe in the Southern Ocean (Atlantic sector), Deep-Sea Res. Pt. II, 58, 2678–2694, 2011.
Lancelot, C., Hannon, E., Becquevort, E., Veth, C., and De Baar, H. J. W.: Modelling phytoplankton blooms and carbon export production in the Southern Ocean: dominant controls by light and iron in the Atlantic sector in Austral spring 1992, Deep Sea Res. Pt. I, 47, 1621–1662, 2000.
Lancelot, C., de Montety, A., Goosse, H., Becquevort, S., Schoemann, V., Pasquer, B., and Vancoppenolle, M.: Spatial distribution of the iron supply to phytoplankton in the Southern Ocean: a model study, Biogeosciences Discuss., 6, 4919–4962, doi:10.5194/bgd-6-4919-2009, 2009.
Laës, A., Blain, S., Laan, P., Achterberg, E. P., Sarthou, G., and De Baar, H. J. W.: Deep dissolved iron profiles in the eastern North Atlantic in relation to watermasses, Geophys. Res. Lett., 30, 1–3, 2003.
Lannuzel, D., Schoemann, V., De Jong, J. T. M., Chou, L., Delille, B., Becquevort, S., and Tison, J.-L.: Iron study during a time series in the western Weddell pack ice, Mar. Chem., 108, 85–95, 2008.
Lösscher, B., De Baar, H. J. W., De Jong, J. T. M., Veth, C., and Dehairs, F.: The distribution of Fe in the Antarctic Circumpolar Current, Deep-Sea Res. Pt. II, 44, 143–187, 1997.
Lin, H., Rauschenberg, S., Hexel, C. R., Shaw, T. J., and Twining, B. S.: Free drifting icebergs as sources of iron to the Weddell Sea, Deep Sea Res. Pt. II, 58, 1392–1406, 2011.
Luther, III. G. W. and Wu, J.: What controls dissolved iron concentrations in the world ocean? – a comment, Mar. Chem., 57, 174–181, 1997.

Marchetti, A. and Cassar, N.: Diatom elemental and morphological changes in response to iron limitation: a brief review with potential paleoeanographic applications, Geobiology, 7, 419–431, 2009.
Martin, J. H. and Fitzwater, S. E.: Iron deficiency limits phytoplankton growth in the north-east Pacific subarctic, Nature, 331, 341–343, 1988.
Martin, J. H., Gordon, R. M., and Fitzwater, S. E.: Iron in Antarctic waters, Nature, 345, 156–158, 1990.
Matano, R. P., Gordon, A. L., Muench, R. D., and Palma, E. D.: A numerical study of the circulation in the northwestern Weddell Sea, Deep-Sea Res. Pt. II, 49, 4827–4841, 2002.
Meredith, M. P., Hughes, C. W., and Foden, P. R.: Downslope convection north of Elephant Island, Antarctica: Influence on deep waters and dependence on ENSO, Geophys. Res. Lett., 30, 1462, doi:10.1029/2003GL017074, 2003.
Middag, R., de Baar, H. J. W., Laan, P., Cai, P. H., and van Ooijen, J. C.: Dissolved manganese in the Atlantic sector of the Southern Ocean, Deep-Sea Res. Pt. II, 58, 2661–2677, 2011a.
Middag, R., Van Slooten, C., de Baar, H. J. W., and Laan, P., Dissolved aluminium in the Atlantic sector of the Southern Ocean, Deep-Sea Res. Pt. II, 58 2647–2660, 2011b.
Middag, R., de Baar, H. J. W., Laan P., and Huhn, O.: The effects of continental margins and water mass circulation on the distribution of dissolved aluminium and manganese in Drake Passage. J. Geophys. Res. 117, C01019, doi:10.1029/2011JC007434, 2012.
Middag, R., de Baar, H. J. W., Klunder, M. B., Laan, P.: Fluxes of dissolved aluminum and manganese to the Weddell Sea and indications for manganese co-limitation, Limnol. Oceanogr., 58, 287–300, 2013.
Mitchell, G. B. and Holm-Hansen, O.: Observations of modelling of the Antartic phytoplankton crop in relation to mixing depth, Deep Sea Res. Pt. A., Oceanographic Research Papers, 38, 981–1007, 1991.
Moore, J. K. and Abbott, M. R.: Surface chlorophyll concentrations in relation to the Antarctic Polar Front: seasonal and spatial patterns from satellite observations, J. Mar. Syst., 37, 69–86, 2002.
Neven, I., Stefels, J., van Heuven, S., De Baar, H. J. W., and Elzinga, J. T. M.: High plasticity in inorganic carbon uptake by Southern Ocean phytoplankton in response to ambient CO_2, Deep-Sea Res. Pt. II, 58 2636–264, 2011.

BGD
10, 7433–7489, 2013

Dissolved Fe across the Weddell Sea and Drake Passage

M. B. Klunder et al.

Naveira Garabato, A. C., McDonagh, E. L., Stevens, D. P., Heywood, K. J., and Sanders, R. J.: On the export of Antarctic Bottom Water from the Weddell Sea. Deep-Sea Res. Pt. II, 49, 4715–4742, 2002.

Orsi, A. H., Nowlin Jr, W. D., and Whitworth III, T.: On the circulation and stratification of the Weddell Gyre, Deep Sea Res. Pt. I, 40, 169–203, 1993.

Planquette, H., Statham, P. J., Fones, G. R., Charette, M. A., Mark Moore, C., Salter, I., Nedelec, F. H., Taylor, S. L., French, M., Baker, A. R., Mahowald, N., and Jickells, T. D.: Dissolved iron in the vicinity of the Crozet Islands, Southern Ocean, Deep-Sea Res. Pt. II, 54, 1999–2019, 2007.

Pollard, R. T., Lucas, M. I., and Read, J. F.: Physical controls on biogeochemical zonation in Southern Ocean. Deep Sea Res. Pt. II, 49, 3931–3950, 2002.

Raiswell, R.: Iceberg-hosted nanoparticulate Fe in the Southern Ocean: Mineralogy, origin, dissolution kinetics and source of bioavailable Fe. Deep-Sea Res. Pt. II, 58, 1364–137, 2011.

Renault, A., Provost, C., Sennechael, N. , Barré, N., and Kartavtseff, A.: Two full-depth velocity sections in the Drake Passage in 2006 – Transport estimates, Deep-Sea Res. Pt. II, 58, 2572–2591, 2011.

Rijkenberg, M. J. A., Gerringa, L. J. A., Laan, P., Schoemann, V., Middag, R., van Heuven, S. M. A. C., van Aken, H. M., De Jong, J. T. M., and De Baar, H. J. W.: Dissolved Fe in the Western Atlantic Ocean: Distribution, Sources, Sinks and Cycling Goldschmidt Conference, August, 2011.

Rutgers vanderLoeff, M., Cai, P., Stimac, I., Bracher, A., Middag, R., Klunder, M. B., and van Heuven, S., ^{234}Th in surface waters: distribution of particle export flux across the Antarctic Circumpolar Current and in the Weddell Sea during the GEOTRACES expedition ZERO and DRAKE. Deep-Sea Res. Pt. II, 58, 2749–2766, 2011.

Sañudo-Wilhelmy, S. A., Olsen, K. A., Scelfo, J. M., Foster, T. D., and Flegal, A. R., Trace metal distributions off the Antarctic Peninsula in the Weddell Sea, Mar. Chem., 77, 157–170, 2002.

Sarthou, G., Timmermans, K. R., Blain, S., and Tréguer, P.: Growth physiology and fate of diatoms in the ocean: a review, J. Sea Res., 53, 25–42, 2005.

Sokolov, S. and Rintoul, S. R.: On the relationship between fronts of the Antarctic Circumpolar Current and surface chlorophyll concentrations in the Southern Ocean, J. Geophys. Res., 112, C07030, doi:10.1029/2006JC004072, 2007.

BGD
10, 7433–7489, 2013

Dissolved Fe across the Weddell Sea and Drake Passage

M. B. Klunder et al.

Title Page
Abstract | Introduction
Conclusions | References
Tables | Figures
◂◂ | ▸▸
◂ | ▸
Back | Close
Full Screen / Esc
Printer-friendly Version
Interactive Discussion

Stuart, K. M. and Long, D. G.: Tracking large tabular icebergs using the SeaWinds Ku-band microwave scatterometer. Deep Sea Res. Pt. II, Topical Studies in Oceanography, 58, 1285–1300, 2011.

Sudre, J., Garçon, V., Provost, C., Sennechael, Huhn, O., and Lacombe, M., Multiparametric analysis of water masses across Drake Passage during ANT-XXIII/3, Deep-Sea Res. Pt. II, 58, 2592–2612, 2011.

Takeda, S.: Influence of iron availability on nutrient composition ratio of diatoms in oceanic waters, Nature, 93, 774–777, 1998.

Timmermans, K. R., Van de Wagt, B., and De Baar, H. J. W.: Growth rates, half-saturation constants, and silicate, nitrate, and phosphate depletion in relation to iron availability of four large, open-ocean diatoms from the Southern Ocean, Limnol. Oceanogr., 49, 2141–2151, 2005.

Thuroćzy, C. E. T., Gerringa, L. J. A., Klunder, M. B., Middag, R., Laan, P., Timmermans, K. R., and De Baar, H. J. W.: Speciation of Fe in the Eastern North Atlantic Ocean, Deep Sea Res. Pt. I, 57, 1444–1453, 2010.

Vancoppenolle, M., Goosse, H., de Montety, A., Fichefet, T., Tremblay, B., and Tison, J.-L., J. Geophys, Res., 115, C02005, doi:10.1029/2009JC005369, 2010.

Well, R., Roether, W., Stevens, D. P.: An additional deep water mass in Drake Passage as revealed by ^{3}He data, Deep-Sea Res. Pt. I, 50, 1079–1098, 2003.

Weppernig, R., Schlosser, P., Khatiwala, S., and Fairbanks, R. G.: Isotope data from ice Station Weddell: implications for deep water formation in the Weddell Sea, J. Geophys. Res., 101, 25723–25739, 1996.

Table 1. Size and volume of diatom species at the Zero Meridian and Eastern Weddell Sea Stations.

	Stations	Biovolume/cell	Percentage of species	
			Large	Small
			(>5000 µm^3) (%)	(<1000 µm^3)(%)
Greenwich Meridian	150	3408	78	5
	167	8436	87	2
	161	8272	88	2
	178	7810	82	2
	Average	6981	84	3
	St deviation	2397	5	1
Eastern Weddell Sea	191	7420	94	5
	193	4506	74	5
	198	2735	49	7
	204	3390	75	7
	210	3240	57	12
	Average	4258	70	7
	St deviation	1882	18	3
Difference*		0.048	0.084	0.018

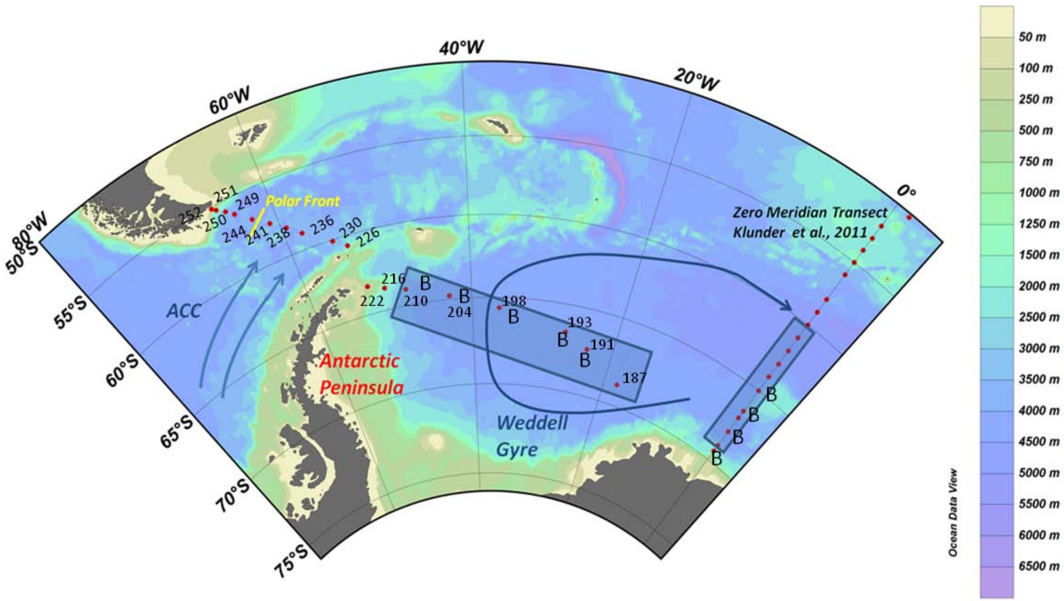

Fig. 1. Sampling region including Weddell Sea and Drake Passage stations (red marked). Also shown are the general flow directions (blue arrows) of the Weddell Gyre and Antarctic Circumpolar Current (ACC) and the position of the Polar Front in the Drake Passage section(yellow). The westward geographic boundary of the Weddell Sea is the Antarctic Peninsula up to Elephant Island, the traditional eastward boundary at Cap Norvegia (12° W). Please be aware that the Weddell Gyre extends far more eastwards to ∼20° E. Northwards of the Weddell Gyre is the Weddell-Scotia Confluence transition zone towards the Scotia Sea, the latter part of the Antarctic Circumpolar Current. The blue shaded boxes show the stations for which nutrient removal is calculated (see main text; Figs. 6 and 7). Stations for which biological (phytoplankton) data is available are marked with a "B" (see text).

BGD
10, 7433–7489, 2013

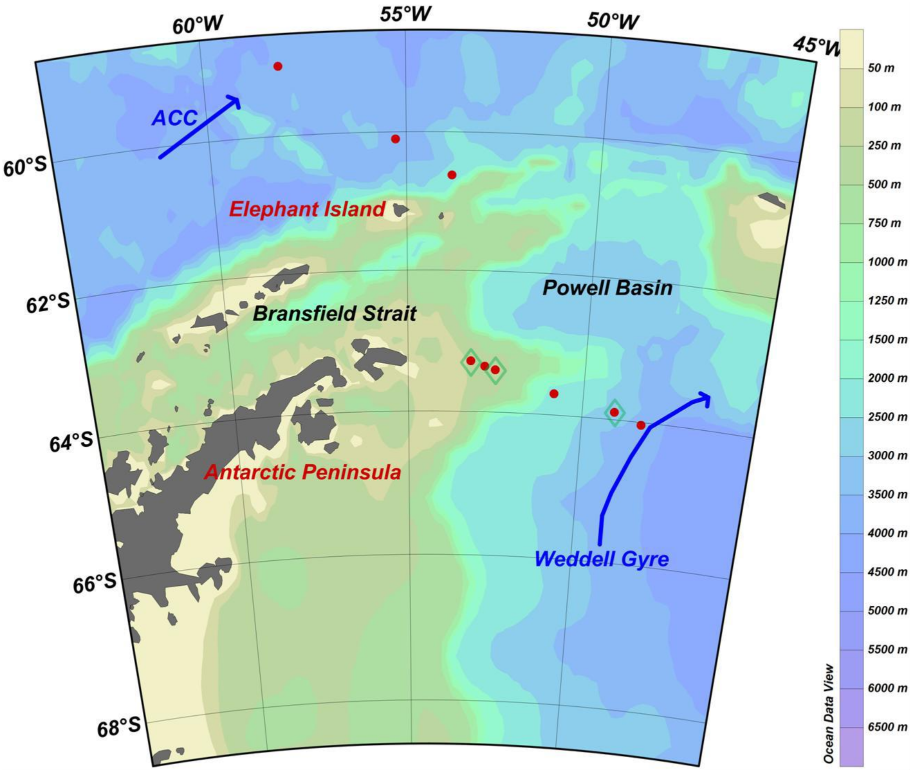

Fig. 2. Overview of Peninsula region at expanded regional scale. Sample stations are indicated with red dots; green diamond marks stations with a few (<5) samples. Flow directions of Weddell Gyre and ACC are indicated schematically with blue arrows.

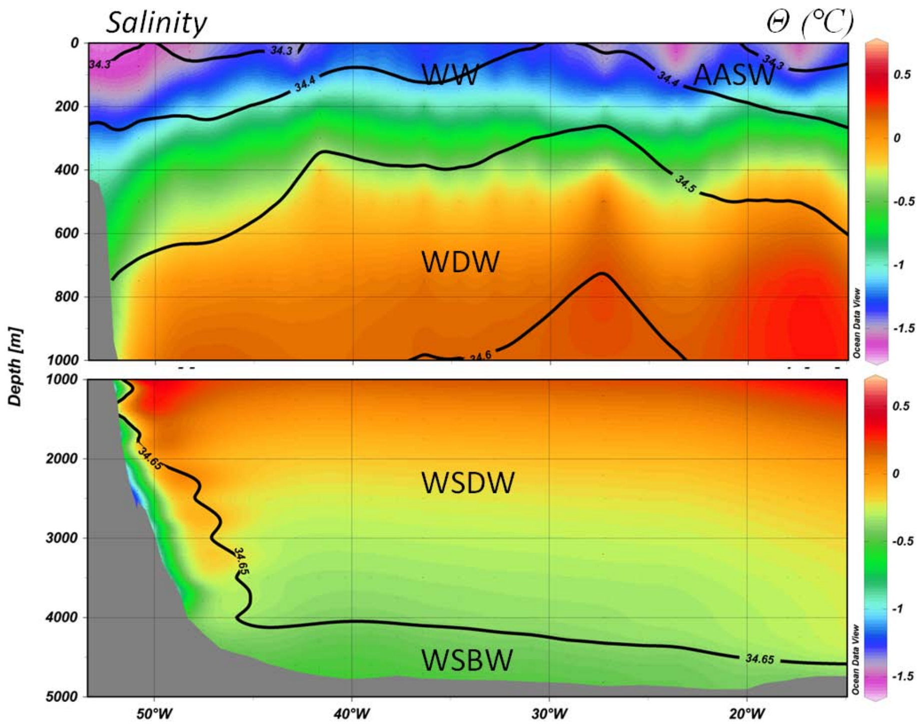

Fig. 3. Potential temperature (color) and salinity (black contour lines) full depth section of the Weddell Sea transect. Approximate location of water masses is indicated.

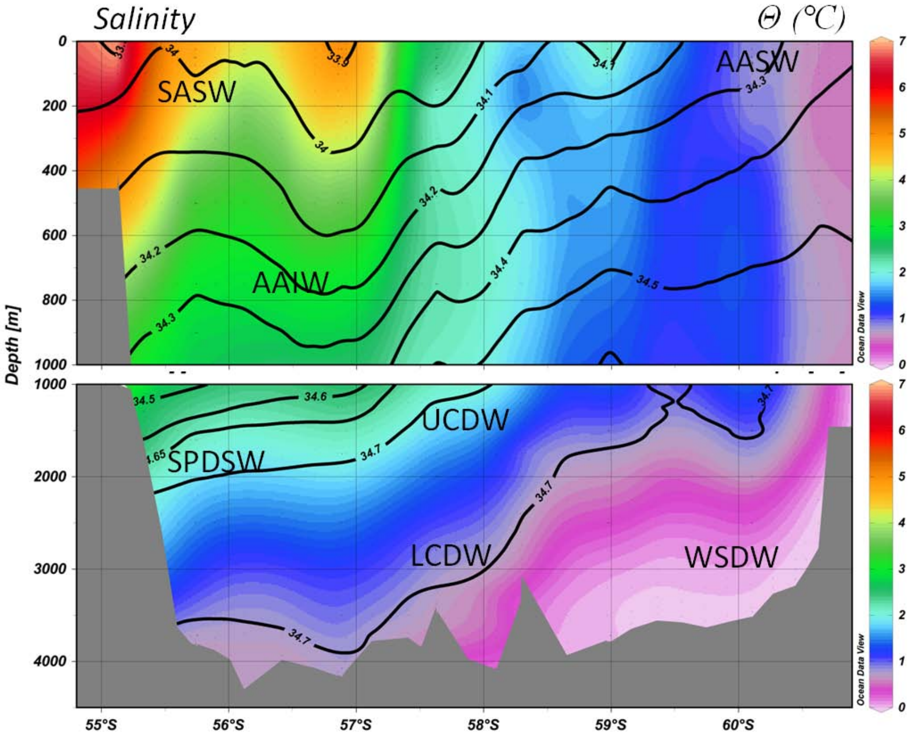

Fig. 4. Potential temperature (color) and salinity (black contour lines) section of the of the Drake Passage transect. Approximate location of water masses is indicated.

BGD
10, 7433–7489, 2013

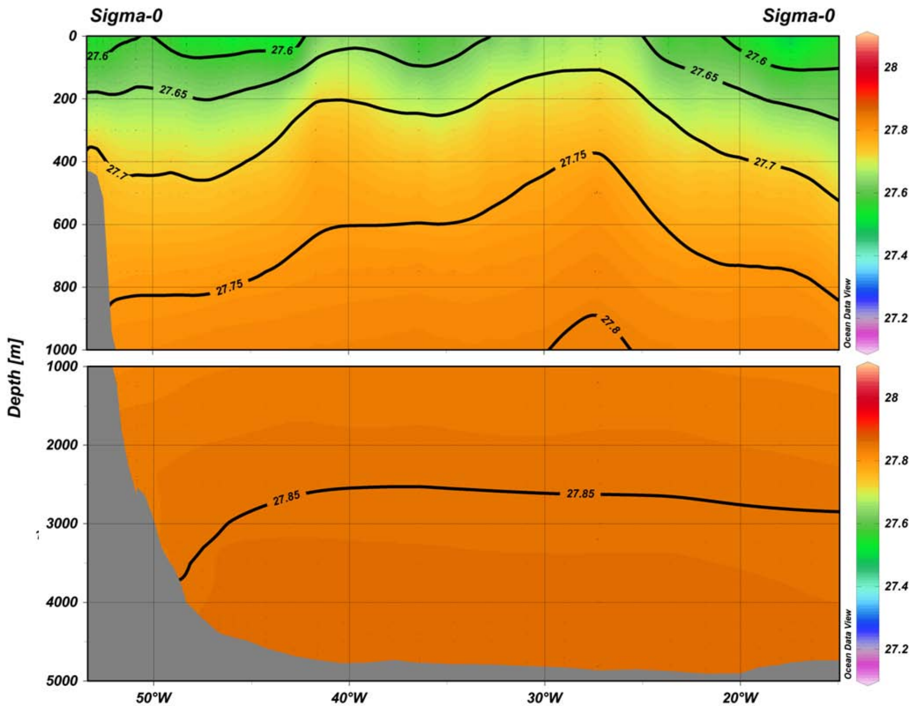

Fig. 5. Section potential density (Sigma theta) versus surface reference level (Sigma-0) of the of the Weddell Sea transect

BGD
10, 7433–7489, 2013

Dissolved Fe across the Weddell Sea and Drake Passage

M. B. Klunder et al.

Title Page
Abstract | Introduction
Conclusions | References
Tables | Figures
◀| |▶
◀ ▶
Back | Close
Full Screen / Esc
Printer-friendly Version
Interactive Discussion

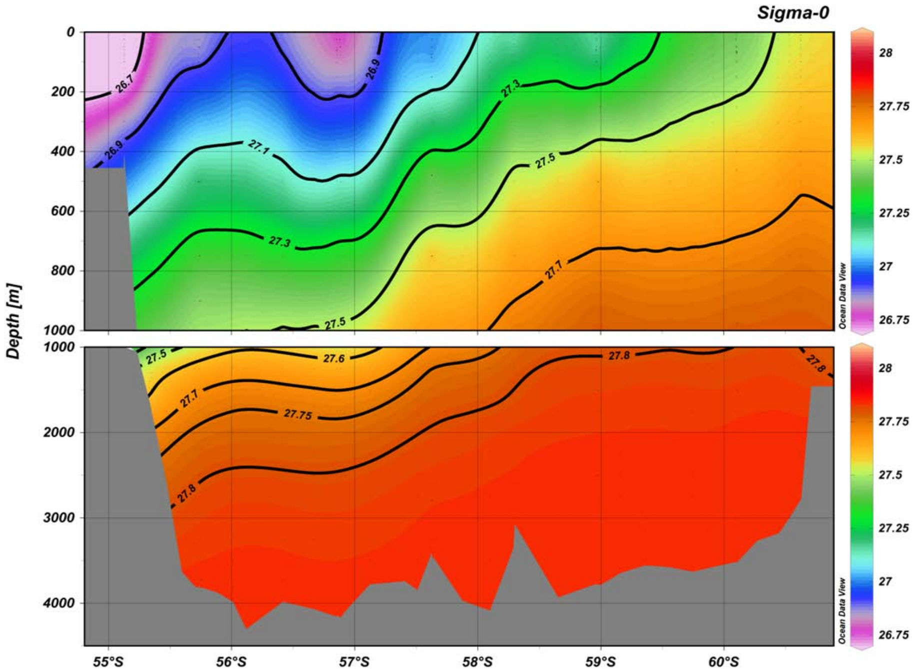

Fig. 6. Section potential density (Sigma-theta) versus surface reference level (Sigma-0) of the of the Drake Passage transect

BGD
10, 7433–7489, 2013

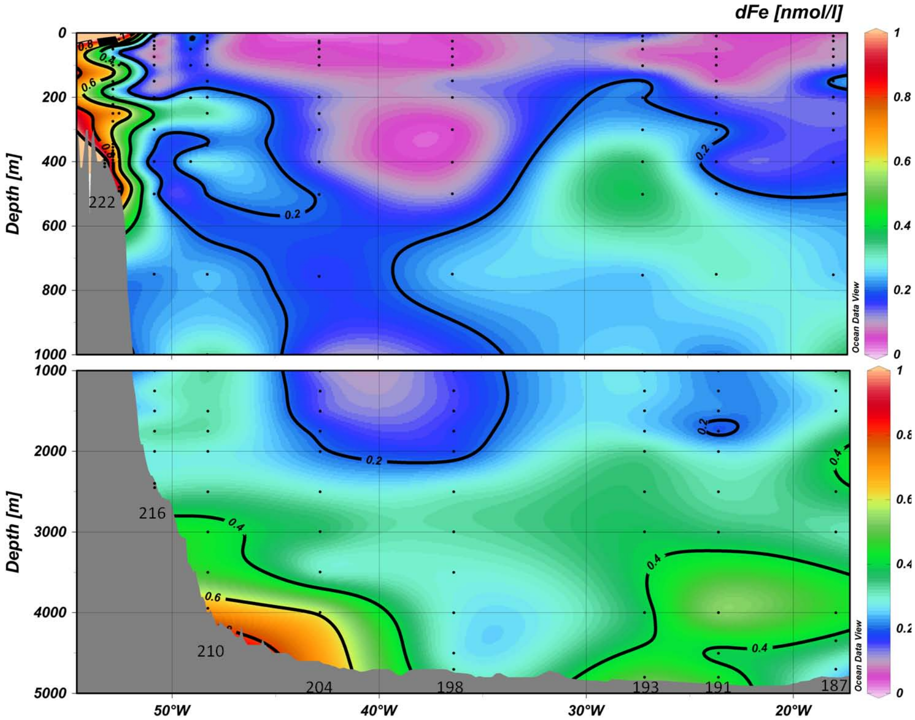

Fig. 7. Section plot of DFe concentrations in the Weddell Sea transect; station numbers 187-216 along horizontal axis.

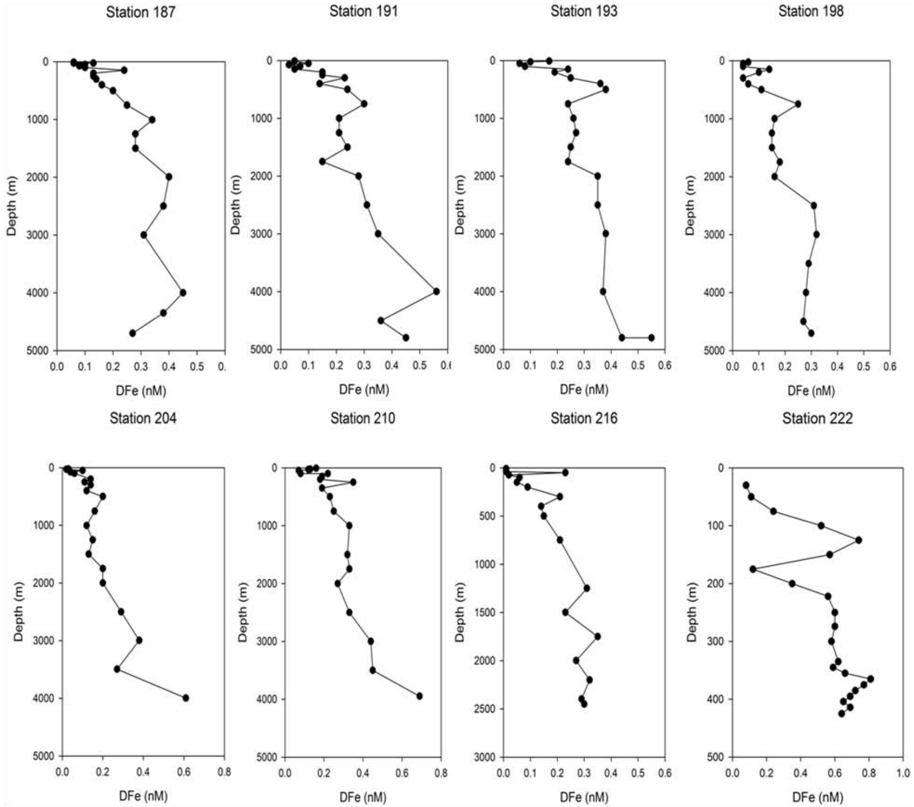

Fig. 8. Vertical profiles of DFe at individual stations of the transect Weddell Sea. Note the different depth and concentration scale.

BGD
10, 7433–7489, 2013

Dissolved Fe across the Weddell Sea and Drake Passage

M. B. Klunder et al.

Title Page
Abstract
Introduction
Conclusions
References
Tables
Figures
◀
▶
Back
Close
Full Screen / Esc
Printer-friendly Version
Interactive Discussion

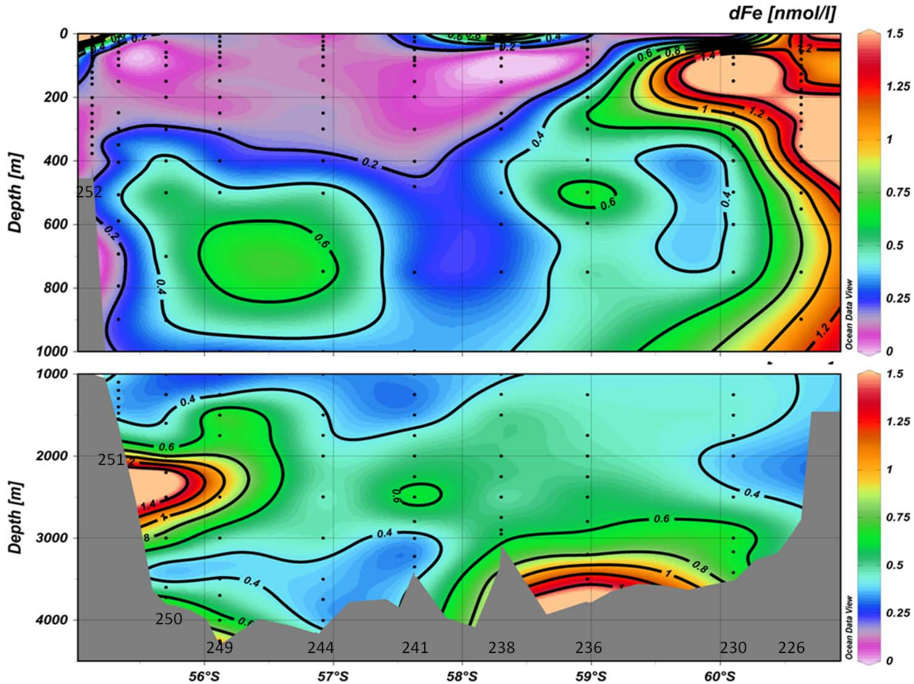

Fig. 9. Section plot of DFe concentrations in the Drake Passage transect. station numbers 226-251 along horizontal axis.

BGD
10, 7433–7489, 2013
Dissolved Fe across the Weddell Sea and Drake Passage
M. B. Klunder et al.

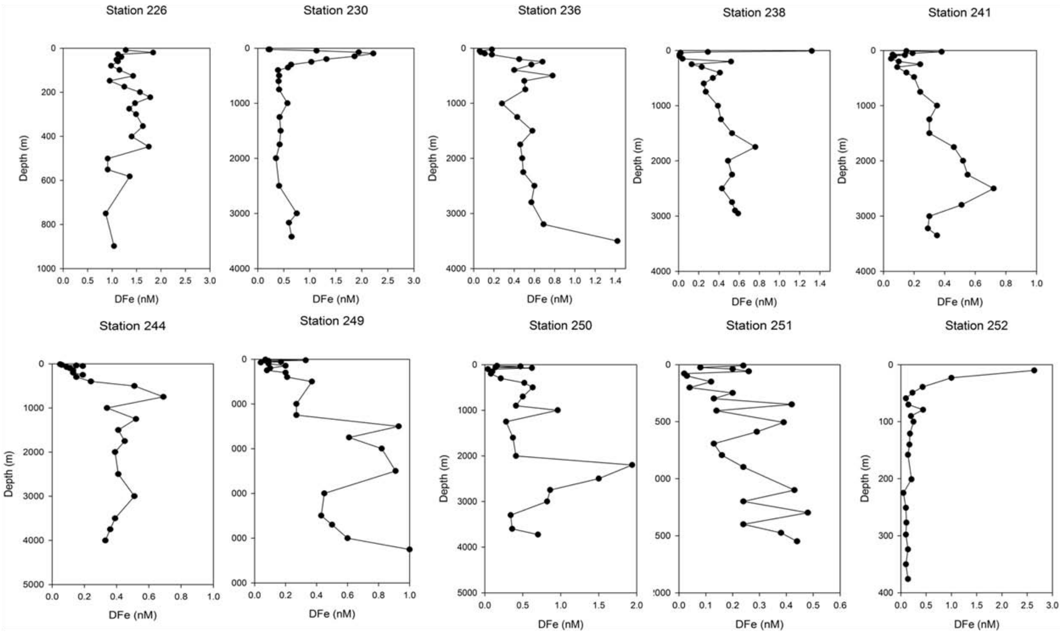

Fig. 10. Vertical profiles of DFe at individual stations of the transect Drake Passage. Note the different depth and concentration scale.

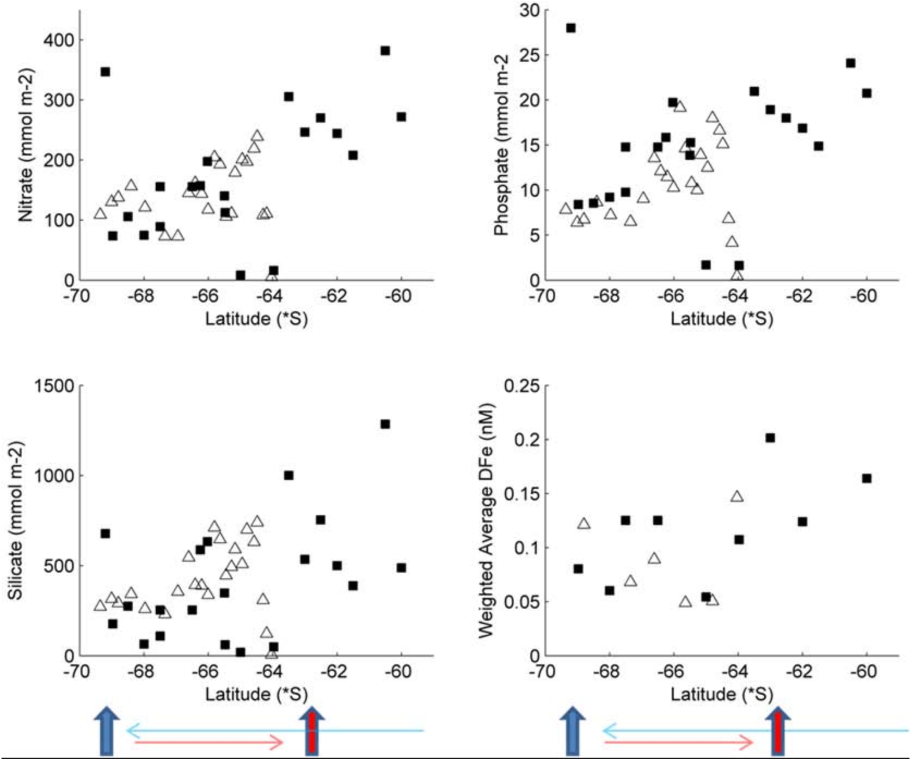

Fig. 11. Removal of nitrate **(a)**, silicate **(b)**, phosphate **(c)** and weighted average DFe **(d)** against latitude for the Weddell Sea transect (open triangles), and the Greenwich meridian transect (filled squares) (Klunder et al., 2012). Nutrients data is available for more stations than DFe data, hence more datapoints. Location of the shelf (500 m depth isobaths) is marked for the Greenwich meridian transect (blue vertical arrow) and the Weddell Sea transect (red vertical arrow). Horizontal light arrows (blue and red) indicate the direction of the ship along the transect. (Please notice that the Greenwich meridian transect is oriented North-South, and the Weddell transect is oriented from SouthEast to Northwest (see Fig. 1a)).

BGD
10, 7433–7489, 2013

Dissolved Fe across the Weddell Sea and Drake Passage

M. B. Klunder et al.

Title Page
Abstract | Introduction
Conclusions | References
Tables | Figures
◀| |▶
◀ ▶
Back | Close
Full Screen / Esc
Printer-friendly Version
Interactive Discussion

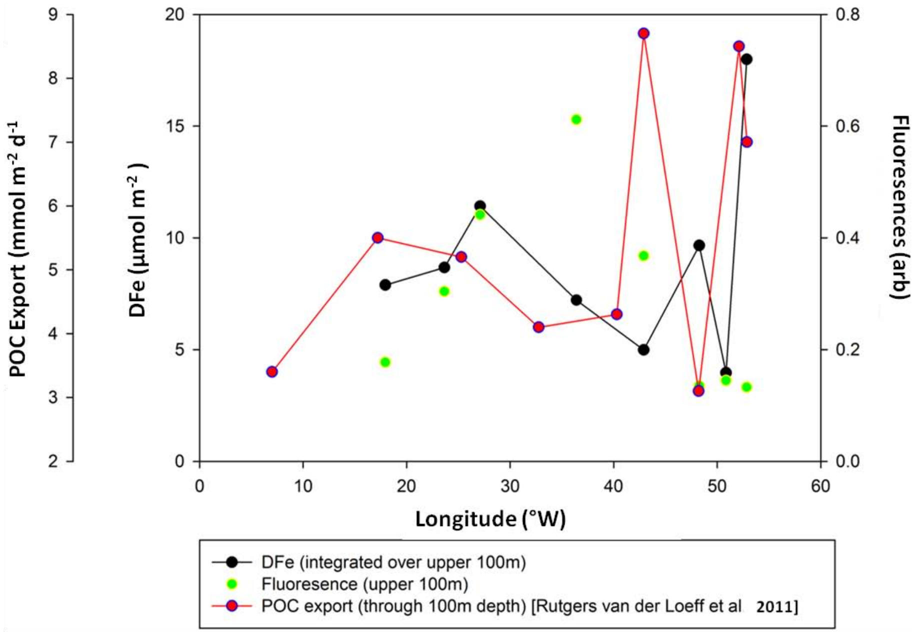

Fig. 12. DFe (integrated over upper 100 m), fluorescence signal (average over upper 100 m) and POC export (through 100 m depth) over the Weddell Sea transect.

BGD
10, 7433–7489, 2013

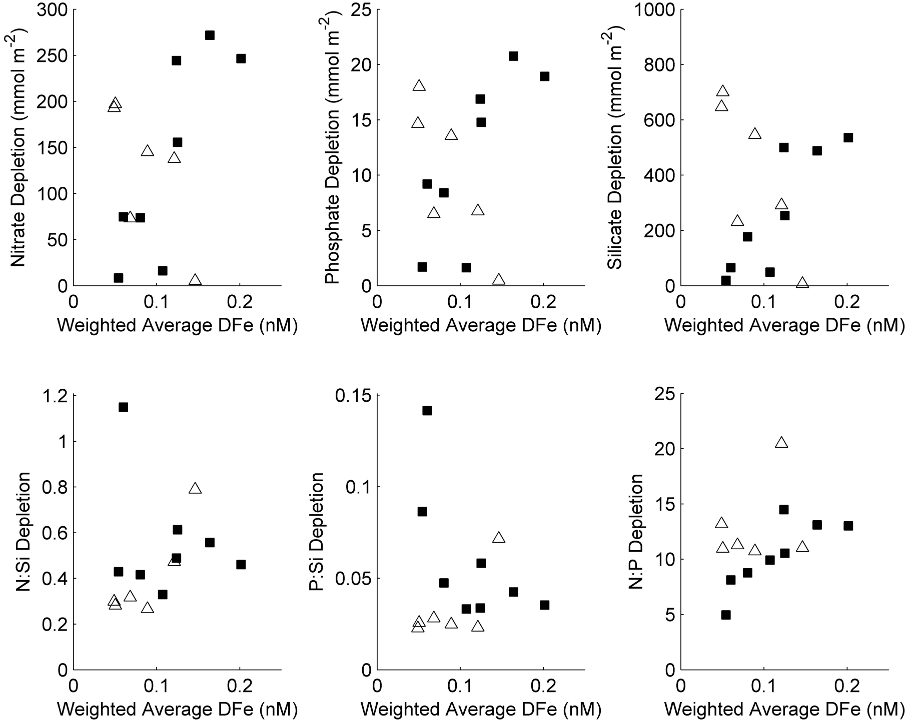

Fig. 13. Removal of nitrate **(a)**, silicate **(b)**, phosphate **(c)** and the removal ratios of N:Si **(d)**, P:Si **(e)** and N:P **(f)** vs. the weighted average DFe concentrations for the Weddell Sea transect (open triangles), and the Greenwich meridian transect (filled squares) (Klunder et al., 2011).

BGD
10, 7433–7489, 2013

Dissolved Fe across the Weddell Sea and Drake Passage

M. B. Klunder et al.

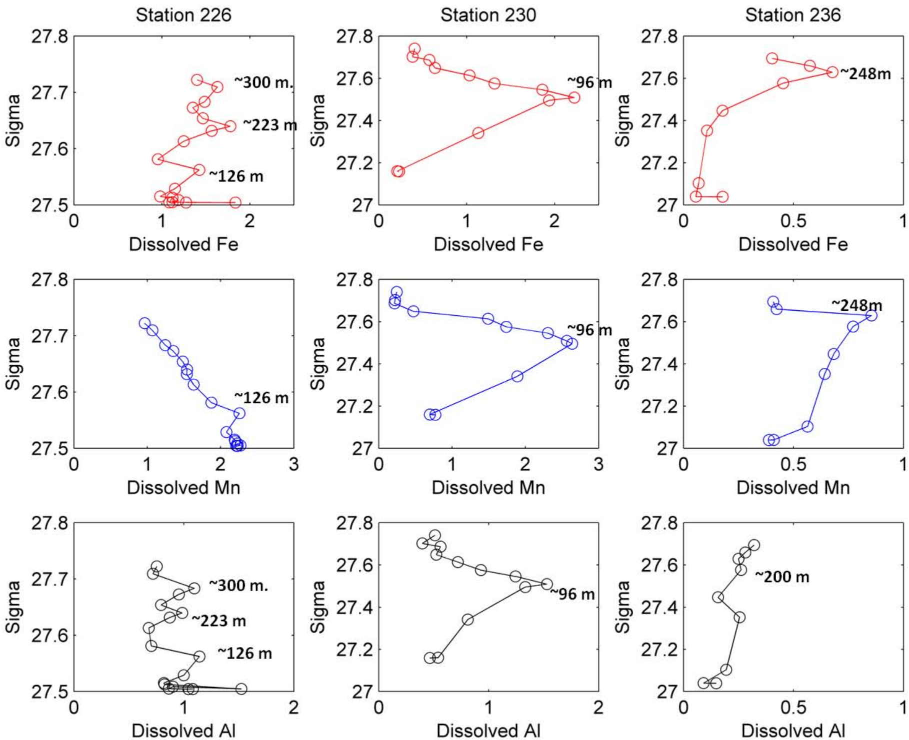

Fig. 14. Sigma theta ($\sigma\theta$) versus Dissolved Fe, Dissolved Mn (Middag et al., 2012) and Dissolved Al (Middag et al., 2012) (nM) for the stations adjacent to Elephant Island (see Fig. 1b). Note the different metal concentration scales for different stations. Also corresponding depths of peak values are shown.

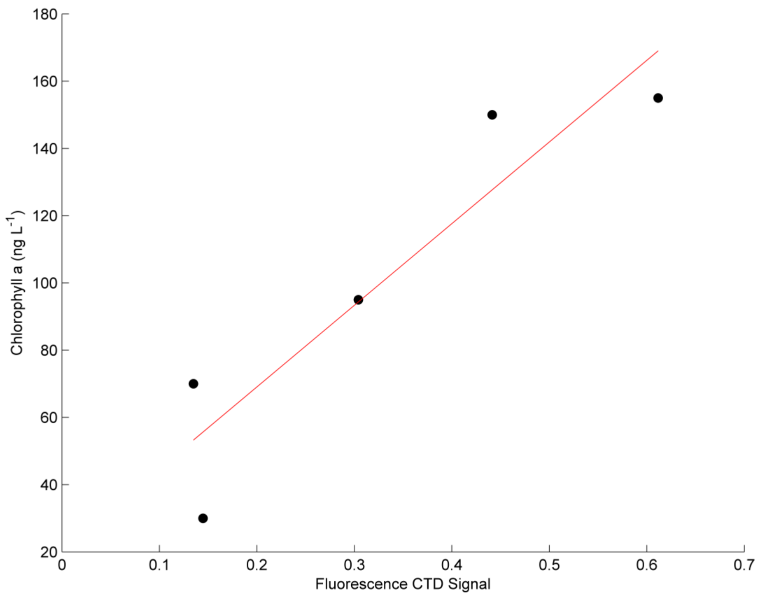

Fig. A1. Correlation between fluorescence signal and Chl for those stations in the Weddell Sea where data for both parameters is available . Linear fit is shown in the figure ($R^2 = 0.85$; $P = 0.01$; $n = 5$).

BGD
10, 7433–7489, 2013

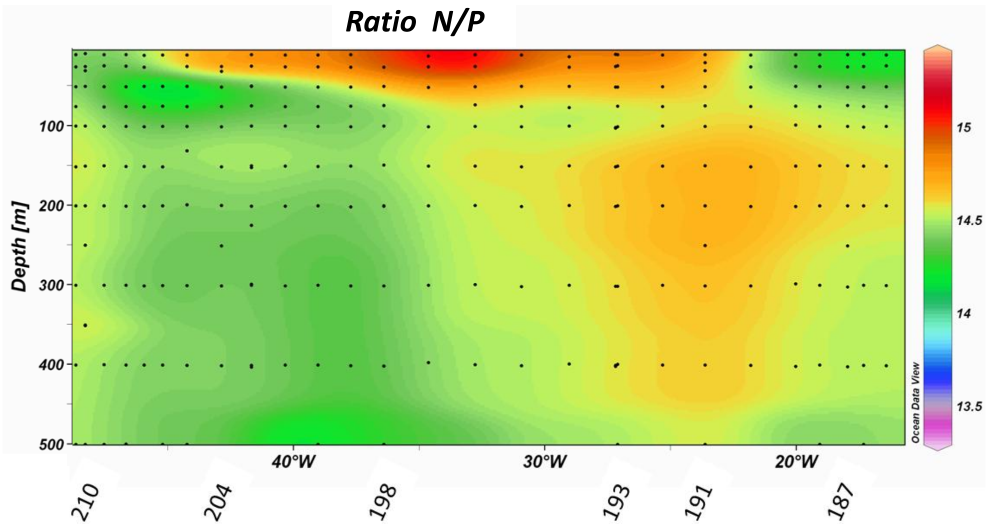

Fig. A2a. Section plot of N:P ratio in the Weddell Sea transect, for that region where a Winter Water Layer is observed and a removal ratio is calculated (∼ 17–∼ 48.5° W). The locations of the stations where DFe data is available and a nutrient removal is calculated are presented.

BGD
10, 7433–7489, 2013

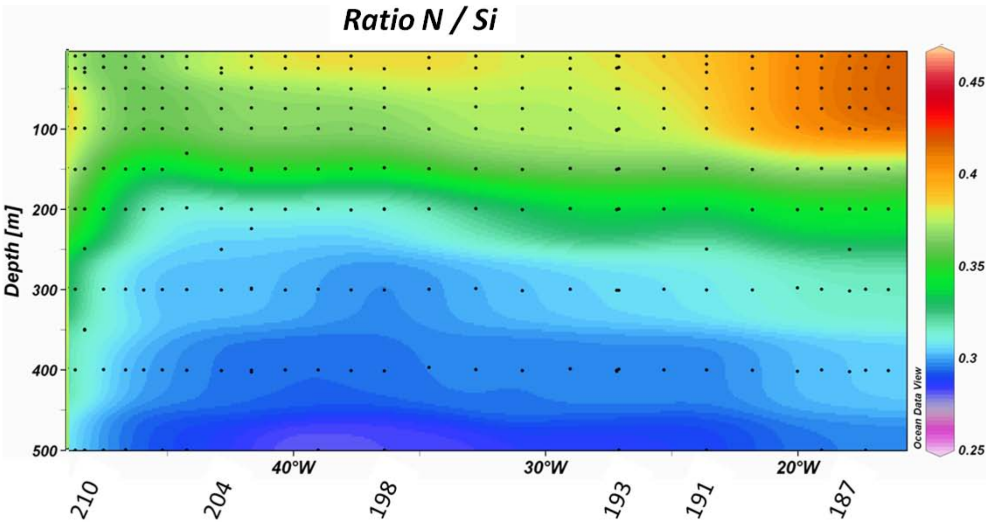

Fig. A2b. Section plot of N:Si ratio in the Weddell Sea transect, for that region where a Winter Water Layer is observed and a removal ratio is calculated (∼ 17–∼ 48.5° W). The locations of the stations where DFe data is available and a nutrient removal is calculated are presented.

BGD
10, 7433–7489, 2013

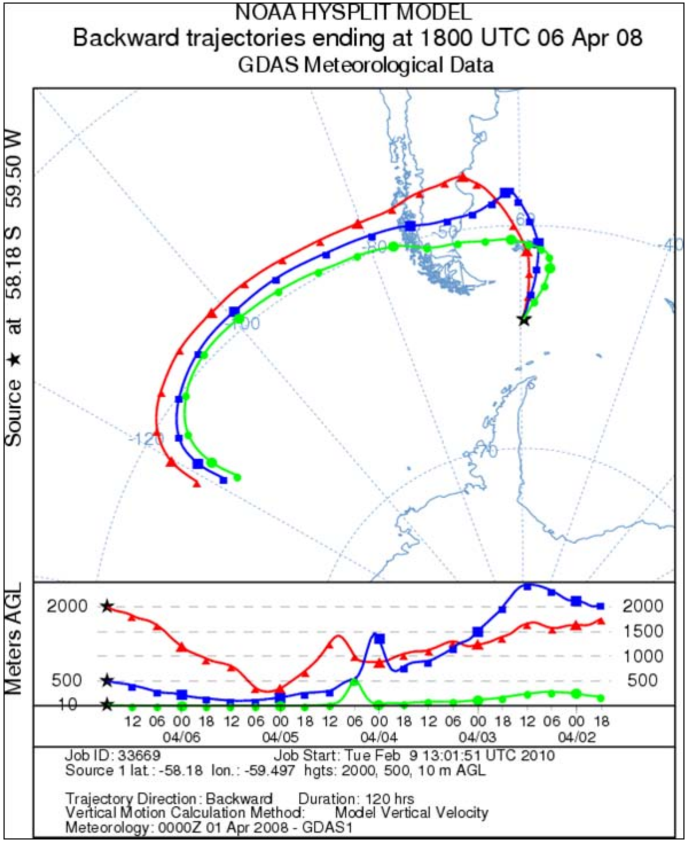

Fig. A3. Five day backwards air-trajectory from station 238, during ANT XXIV.

BGD
10, 7433–7489, 2013

Dissolved Fe across the Weddell Sea and Drake Passage

M. B. Klunder et al.